Conserved mammalian muscle mechanics during eccentric contractions

Roger W. P. Kissane[1*] and Graham N. Askew[2*]

[1] Department of Musculoskeletal & Ageing Science, University of Liverpool, The William Henry Duncan Building, 6 West Derby Street, Liverpool L7 8TX, UK

[2] School of Biomedical Sciences, University of Leeds, UK

*Correspondence to: r.kissane@liverpool.ac.uk and g.n.askew@leeds.ac.uk

Funding: This research was supported by a BBSRC Project Grant (BB/R016917/1) to GNA. This work was also supported by an internal funding scheme funded by the Wellcome Trust Institutional Strategic Support Fund grant (204822/Z/16/Z) and awarded to RWPK by the Faculty of Health and Life Sciences, University of Liverpool.

Running Title: Conserved mammalian muscle mechanics during eccentric contractions

Key words: Force Velocity, Muscle Mechanics, Scaling, Titin, Lengthening

Key Point Summary

- The capacity of skeletal muscle to generate mechanical work and absorb energy is underpinned by the force-velocity relationship
- Despite identification of the lengthening (eccentric) force-velocity relationship over 80 years ago no comprehensive study has been undertaken to characterise this relationship in skeletal muscle
- We show that the biphasic force response seen during active muscle lengthening is conserved over three orders of magnitude of mammalian skeletal muscle mass
- Using mice with a small deletion in titin we show that part of this biphasic force profile in response to muscle lengthening is reliant on normal titin activation
- The rate of force development during muscle stretch may be a more reliable way to describe the forces experienced during eccentric muscle contractions compared to the traditional hyperbolic curve fitting, and functions as a novel predictor of force-velocity characteristics that may be used to better inform hill-type musculoskeletal models and assess pathophysiological remodelling

Abstract

Skeletal muscle has a broad range of biomechanical functions, including power generation and energy absorption. These roles are underpinned by the force-velocity relationship, which comprises two distinct components: a concentric and an eccentric force-velocity relationship. The concentric component has been extensively studied across a wide range of muscles with different muscle properties. However, to date little progress has been made in accurately characterising the eccentric force-velocity relationship in mammalian muscle with varying muscle properties. Consequently, mathematical models of this muscle behaviour are based on a poorly understood phenomenon. Here we present a comprehensive assessment of the concentric force-velocity and eccentric force-velocity relationships of four mammalian muscles (soleus, extensor digitorum longus, diaphragm and digastric) with varying biomechanical functions, spanning three orders of magnitude in body mass (mouse, rat and rabbits). The force velocity relationship was characterised using a hyperbolic-linear equation for the concentric component a hyperbolic equation for the eccentric component, while also measuring the rate of force development in the two phases of force development in relation to eccentric lengthening velocity. We demonstrate that despite differences in the curvature and plateau height of the eccentric force-velocity relationship, the rates of relative force development were consistent for the two phases of the force-time response during isovelocity lengthening ramps, in relation to lengthening velocity, in the four muscles studied. Our data support the hypothesis that this relationship depends on crossbridge and titin activation. Hill-type musculoskeletal models of the eccentric force-velocity relationship for mammalian muscles should incorporate this biphasic force response.

Introduction

Skeletal muscles have a broad range of biomechanical functions: muscles may generate force whilst shortening to generate mechanical work, functioning as a motor; other muscles may primarily be active during muscle lengthening, dissipating mechanical energy and functioning as a brake; and others may operate as tension struts, generating force without undergoing any change in length (Azizi, 2014; Lai *et al.*, 2019; Charles *et al.*, 2022; Kissane *et al.*, 2022; Usherwood, 2022). The capacity of skeletal muscle to generate and absorb mechanical work and power is underpinned by the force-velocity relationship (Askew, 2023). This relationship comprises two distinct components: a shortening (or concentric) force-velocity relationship (Hill, 1938) and a lengthening (or eccentric) force-velocity relationship (Edman *et al.*, 1978).

While the shortening force-velocity relationship has been extensively investigated across a range of phenotypically distinct muscles (Barclay, 1996; Askew & Marsh, 1997), scaling relationships (Pellegrino *et al.*, 2003) and even in response to pathophysiological remodelling (Warren *et al.*, 2020; Espino‐Gonzalez *et al.*, 2021), the lengthening force-velocity relationship has been comparably less well studied (Mendoza *et al.*, 2023). Despite identification of the relationship over 80 years ago (Katz, 1939) no comprehensive study has been undertaken to characterise this relationship in skeletal muscle. Previous studies have used different methodological approaches; e.g. some studies have used isovelocity (velocity clamped) contractions while others have used isotonic (force-clamped) contractions, which yield different force profiles and consequently different force-velocity relationships (Woledge *et al.*, 1985). Some investigations have used rather small sample sizes (Joyce *et al.*, 1969), or been completed at non-physiological temperatures (Lännergren, 1978; Edman, 1988; Alcazar *et al.*, 2019) and carried out using a variety of species (mammalian, amphibians, and crustacean) rendering much of the data available difficult to collate to obtain a generalised understanding of muscle functional behaviour (Alcazar *et al.*, 2019). This is problematic as skeletal muscles function eccentrically across a number of locomotor behaviours like walking (Gillis *et al.*, 2005; Lai *et al.*, 2019), flying (Askew & Marsh, 2001) and feeding (Mayerl *et al.*, 2021). Our limited understanding of this complex behaviour means that estimates of whole motor systems through Hill-type musculoskeletal models are potentially misrepresentative of their true function. Additionally, these principles form the basis of our understanding and investigation of motor control strategies, where for example muscle spindles are thought to be sensitive to not only muscle lengthening velocity but also force generation (Blum *et al.*, 2017; Blum *et al.*, 2020; Kissane *et al.*, 2022, 2023).

The lack of extensive progress in characterising the eccentric force-velocity relationship is perhaps in part due to the complex nature of the muscle force response to active lengthening. It has long been known that muscles undergoing active lengthening produce a dynamic biphasic force response (Joyce *et al.*, 1969; Krylow & Sandercock, 1997; Pinniger *et al.*, 2006; Herzog, 2014; Herzog *et al.*, 2016; Weidner *et al.*, 2022). This biphasic force response (Appendix Fig. 1) comprises a phase of rapid force-development (phase-1) and a phase of slow force-development (phase-2). This complex phenomenon is thought to arise from two distinct mechanical processes. Firstly, the initial rapid phase-1 response is hypothesised to arise from elevated strain of attached cross-bridges, after which the detachment of myosin heads leads to the transition into the shallower phase-2 force response (Tomalka *et al.*, 2020, 2021; Weidner *et al.*, 2022; Tomalka, 2023). The phase-2 force response is thought to be linked to increased strain of non-crossbridge, parallel elastic elements (Ramsey *et al.*, 2010; Tomalka, 2023). There is little known about the rate of force development in these two phases in relation to lengthening velocity, or how or whether this relationship differs between muscles of distinctive phenotypes, or as a result of scaling in relation to body mass. Hence, we have set out to undertake the most comprehensive assessment of eccentric muscle contractile properties to date.

Firstly, we investigated the eccentric response of the phenotypically distinct fast extensor digitorum longus (EDL) and slow soleus (SOL) muscles from the mouse. Despite the comprehensive characterisation of the distinct shortening force-velocity (concentric) properties of these muscles, little is known of the eccentric force-velocity relationship of these two muscles and, specifically, whether there is variation in the rate of force development during phases 1 and 2. When skinned muscle fibres of differing fibre phenotype were actively lengthened they produced comparable steady-state forces and power output (Linari *et al.*, 2004). To achieve this, slow fibres recruit more myosin head attachments, to make up for the difference in initial isometric force (Linari *et al.*, 2004). It is thought that the force enhancement contributed to by contractile elements is greater in the SOL than in the EDL, and that the non-contractile contribution to force enhancement is greater in the EDL than the SOL (Ramsey *et al.*, 2010). These mechanistic differences in active lengthening are thought to lead to differences in the rate of force development during stretch (Hessel & Nishikawa, 2017) between phenotypically different muscles. Therefore, we hypothesise that, like phenotypically distinct skinned fibres, there may exist differences in the classical force-velocity relationship between the SOL and EDL (Linari *et al.*, 2004). In addition, we expect that given the proposed differences in contribution of the contractile and non-contractile elements

(Prado *et al.*, 2005) to the SOL and EDL during eccentric contractions, that both the rates of force development during phase-1 and phase-2 will differ between the two muscles.

In addition to the EDL and SOL from the mouse, we also investigated the eccentric contractile properties of the diaphragm (DIA) muscle from the rat and the digastric (DIG) muscle from the rabbit, extending the range in body mass of the species studied to cover three-orders of magnitude. These anatomically and functionally diverse examples of mammalian muscle provide a unique opportunity to test if this biomechanical phenomenon is conserved between species. We hypothesise that the biphasic force-development profile will be conserved between these mammalian species, and that they may present with comparable rates of force enhancement across a range of lengthening velocities.

Finally, as mentioned previously, the rapid phase-1 force development profile is thought to be the response to elevated strain of attached cross-bridges (Tomalka *et al.*, 2020, 2021; Weidner *et al.*, 2022; Tomalka, 2023), with the phase-2 force response thought to be linked to increased strain of non-crossbridge parallel elastic elements (De Ruiter *et al.*, 2000; Ramsey *et al.*, 2010; Tomalka, 2023). Recent work has shown that titin plays an important role in both passive and active muscle properties, contributing to force enhancement and depression during lengthening and shortening contractions (Tahir *et al.*, 2020). It is therefore plausible that titin plays an important role in the rate of force development during eccentric contractions. Therefore, we have utilised the muscular dystrophy with myositis (mdm) mouse model (Powers *et al.*, 2016; Tahir *et al.*, 2020) with impaired titin activation to investigate the potential contribution of titin to biphasic force development response. It's previously been shown that cross-bridge kinetics are relatively unaffected in mice with mdm (Tahir *et al.*, 2020), therefore we hypothesise that the impaired titin function in the mdm mice will not affect the phase-1 portion of the eccentric force response. However, it is likely to directly impair the phase-2 portion of the eccentric force response, given it has been associated mechanism with non-crossbridge elastic elements.

In summary, we show that the dynamic two-phase force development response of skeletal muscle to active lengthening has a strong, velocity-dependent relationship across all four mammalian muscles. We provide evidence for a novel predictor of force-velocity characteristics, specifically, the rate of force developed during eccentric lengthening, which may be used to better inform Hill-type musculoskeletal models and assess pathophysiological remodelling. Our data also show that the second-phase shallow rate of force development during eccentric contractions is dependent on normal titin activation, but the rapid (phase-1) response is not.

Methods

Ethical Approval

All experimental procedures were performed in accordance with the UK animal scientific procedures act (1986) and approved by the University of Leeds Animal Welfare (PPL: PA1BA29DF) and Ethical Review Committee. This work conforms to the ethical requirements outlined by the journal, and is presented in accordance with guidelines for animal work (Grundy, 2015; Percie du Sert *et al.*, 2020).

Animals

Twenty-one in-house male C57B6 mice (25.06 ± 1.90g), five in-house male Wistar rats (254 ± 10g) and eight male New Zealand white rabbits (Envigo) (2638 ± 85g) were used in this study. Animals were housed under a 12 hour light:dark cycle at 21 °C and had *ad libitum* access to food and water.

Ex-vivo muscle preparation

Both mice and rats were culled using approved schedule 1 methods. The hindlimb of the mouse and the whole rat DIA were transferred to chilled (4°C), oxygenated (95% O_2, 5% CO_2) Krebs-Henseleit solution [117 NaCl, 4.7 KCl, 2.5 $CaCl_2$, 1.2 $MgSO_4$, 24.8 $NaHCO_3$, 1.2 KH_2PO_4 and 11.1 glucose; concentrations in mmol L^{-1}] (Burton, 1975). The whole SOL and EDL were dissected free and aluminium foil clips were attached to the proximal and distal ends of the muscles, with no free tendon left in series (Askew & Marsh, 1997). The rat DIA was pinned out at approximately resting length, and a medial section of the costal diaphragm (width 4-5mm) was dissected maintaining a rib at the proximal end, and a stainless-steel ring was sutured to the central tendon (Warren *et al.*, 2020). The SOL, EDL and DIA were suspended vertically in a flow-through Perspex chamber filled with circulating, oxygenated Krebs–Henseleit solution at 37±0.5°C. Muscles were attached to an ergometer (series 300B-LR; Aurora Scientific Inc., London, Ontario, Canada) via a lightweight stainless-steel rod and muscle length was altered using a micromanipulator. Muscles were left for 30 mins to thermo-equilibrate and recover from the dissection. Parallel platinum electrodes were placed inside the chamber on either side of and parallel to the muscle.

In-situ muscle preparation

Rabbits were anaesthetised with a subcutaneous injection of ketamine (Ketavet, Zoetis; 50mg/kg) and xylazine (Rompun, Bayer; 5mg/kg). Following confirmation of anaesthetic plane, an intravenous canula was implanted to deliver a maintenance dose of ketamine and xylazine throughout the experiment. The DIG muscle was exposed via an incision running the length of the dorsal aspect of the jaw. A 3mm hole was drilled through the mandible and a custom 3D printed mould was screwed to the bone and attached to a custom rig to allow for muscle length to be changed. The distal end of the DIG was sutured to a stainless-steel loop with silk suture (3-0, LOOK Braided suture) and hooked onto the ergometer (305B-LR; Aurora Scientific Inc.). Parallel platinum wires (0.4mm diameter) were implanted into the DIG muscle using a 25-gauge needle and sutured into place. The rabbit was left for 30 minutes to recover from electrode implantation, prior to beginning the muscle mechanical experiments. Throughout the experiment the rabbit's body temperature was maintained at 37°C (Animal Temperature Controller 2000, WPI) and the muscle was regularly irrigated with warmed (37°C) saline. Following completion of the experiment rabbits were culled with an overdose of pentobarbital.

Isometric muscle properties

All muscles were subjected to a series of isometric twitches (supramaximal stimulus of 0.2ms pulse) and muscle lengths were incrementally increased to find the optimal length of force generation (L_0). Maximal isometric tetanic force (P_0) at L_0 was determined using a train of stimuli delivered at 150 Hz for 250 ms for the SOL, at 250 Hz for 200 ms for the EDL, at 200 Hz for 200 ms for the DIA, and 200 Hz for 300 ms for the DIG. Data were sampled at 2 kHz during isometric twitch kinetics. From these data the twitch-rise times and maximal isometric tetanic stress were calculated.

Force-velocity characteristics

The concentric force-velocity relationship of the SOL, EDL, DIA and DIG were determined using a series of isotonic afterload contractions across a range of forces (5-80% of P_0, Fig. 1A, Appendix Figs. 1,2) (Kissane *et al.*, 2018), with data sampled at 2 kHz. Velocity and force were measured as the muscle shortened across L_0 (Fig. 1A, Appendix Figs. 1,2) and the force-velocity relationship was determined by fitting a hyperbolic-linear function (Marsh & Bennett, 1986) to the data (Equation 1). The maximal shortening velocity at zero force (V_{max}), expressed relative to fibre length (FL) for the SOL, EDL, DIA and DIG, was calculated. Peak instantaneous isotonic power

($\dot{W}_{max}$) and the power ratio ($\dot{W}_{max}/P_0V_{max}$), were also determined from the fitted force-velocity relationship.

$$V = \frac{B\left(1-\frac{P}{P_0}\right)}{\left(A+\frac{P}{P_0}\right)+C\left(1-\frac{P}{P_0}\right)} \quad (1)$$

where P/P_0 is relative force and *A, B* and *C* are coefficients. The lengthening force-velocity relationship of the SOL, EDL, DIA and DIG was determined using isovelocity lengthening ramps (Fig. 1B). The SOL, EDL, DIA and DIG were lengthened by 2mm, 1mm, 3mm and 2mm respectively, symmetrically spanning L_0 (Fig. 1C-D). Force and velocity were averaged across L_0 (selecting ±1% muscle length) and used to plot the eccentric force velocity relationship. Muscles were lengthened at velocities up 60% of V_{max}, and the data was sampled at 5 kHz. The lengthening force-velocity relationship was fit with a hyperbolic function (Alcazar *et al.*, 2019) (Equation 2). Coefficients D and E were derived which describe the plateau height (D) and curvature (E) of the relationship (Appendix Fig. 3).

$$P = \frac{E-DV-2V}{E-V} \quad (2)$$

Titin mutant mice

Raw eccentric ramp data were taken from Uzma et al (Tahir *et al.*, 2020). Briefly, muscular dystrophy with myositis (mdm) and wild-type (wt) soleus muscles were subjected to eccentric ramps over a 200ms period, varying the muscle amplitude from +10% to -10%, +8% to -8%, +6% to -6%, +4% to -4%, +2% to -2% of L_0, covering a range of velocities from 0.2-1ML.s^{-1}. Raw data from these experiments were used to calculate the rates of force development in phases 1 and 2 during the eccentric ramp.

Statistics

All data processing and figures were plot using Igor Pro 8 (V8.0.4.2). One-way ANOVAs were completed using SPSS 28 (28.0.1.1), where significance was detected post-hoc comparisons were made using the Bonferroni correction and the threshold for statistical significance set to $P<0.05$. Repeated measures correlations (Bakdash & Marusich, 2017) were undertaken using CRAN R: https://cran.r-project.org/web/packages/rmcorr/ in R (Team, 2010). Least-squares regression slopes between the rate of force development and lengthening velocity were determined for pooled data to

233 determine if significant differences existed between the slopes when accounting for passive force
234 (McFarlane *et al.*, 2016; Kissane *et al.*, 2019). All data are presented as mean ± standard deviation.

Results

Phenotypically distinct muscles from the mouse have distinct eccentric force-velocity characteristics.

The shortening force-velocity characteristics for the mouse EDL and SOL have been comprehensively described in the literature (Luff, 1981; Barclay, 1996; Askew & Marsh, 1997; Askew *et al.*, 1997). Our data presented here (Fig. 2A, D, Table 1) show the EDL to have a significantly greater V_{max} (14.1 ± 1.8 FL s^{-1} *vs.* 7.0 ± 0.6 FL s^{-1}, t(19)= -12.967, P<0.001), a higher power ratio (0.128 ± 0.014 *vs.* 0.089 ± 0.008, t(19)=-7.515, P<0.001), and greater $\dot{W}_{max}$ (402.6 ± 108.2 W kg^{-1} *vs.* 120.0 ± 32.6 W kg^{-1}, t(19)=-8.551, P<0.001) compared to the SOL. These values are comparable to previously published values (Luff, 1981; Askew & Marsh, 1997; Holt & Askew, 2012). In addition to the significantly different isometric twitch kinetics and isotonic shortening profiles (Table 1) the EDL and SOL present with significantly different eccentric force-velocity profiles (Fig. 2A, D, Table 2) with a significantly lower plateau (D coefficient; -0.500 ± 0.039 vs. -0.313 ± 0.063, t(19)=8.082, P<0.001) and lower degree of curvature of this relationship (E coefficient; 0.571 ± 0.313 vs. 0.289 ± 0.117, t(19)=-2.788, P=0.012) in EDL compared to SOL.

As previously mentioned, during the isovelocity ramp the force response presents with a biphasic profile (Joyce *et al.*, 1969; Krylow & Sandercock, 1997; Herzog, 2014; Herzog *et al.*, 2016; Weidner *et al.*, 2022) (Fig. 1|B, Appendix Fig. 1,2), comprising a phase of rapid force-development (phase-1) and a phase of slow force-development (phase-2). Looking specifically at the rate of force development during phase-2 as the eccentric ramp crosses L_0, there is a significantly strong relationship between the rate of force development and the absolute velocity of lengthening for the EDL (r_{rm} (24) = -0.9746, 95% CI [-0.9887, -0.9433], p<0.001, Fig. 2B) and for the SOL (r_{rm} (37) = -0.9750, 95% CI [-0.9869, -0.9525], p<0.001, Fig. 2B) with the rate of change of force increasing with increasing velocity of stretch. This significantly strong relationship is also evident during the phase of rapid force development, i.e. phase-1, (Fig. 1B, Appendix Fig. 1,2) in both the EDL (r_{rm} (24) = -0.9794, 95% CI [-0.9909, -0.9540], p<0.001, Fig. 2C) and SOL (r_{rm} (37) = -0.9907, 95% CI [-0.9951, -0.9821], p<0.001, Fig. 2C) muscles, with the rate of change of force increasing with increasing velocity of stretch. When eccentric velocity is normalised to the muscle-specific V_{max}, these significantly strong relationships remain (Fig. 2E, F).

The rate of force development during eccentric contractions scales across muscles from species covering three orders of magnitude in body mass.

In addition to the EDL and SOL from the mouse, we have also investigated the eccentric contractile properties of the DIA muscle from the rat and the DIG muscle from the rabbit, extending the range in body mass of the species studied to cover three-orders of magnitude (Fig. 3A). Not only are these muscles significantly different in mass (ANOVA $F_{3,28}$=349.755, P<0.001, Fig. 3B), they are also phenotypically distinct (Askew & Marsh, 1997; Warren *et al.*, 2020) (Fig. 3C), and are anatomically divergent with a range of relative fibre-to-muscle lengths (Dantuma & Weijs, 1980; Altringham & Young, 1991; Askew & Marsh, 1997) (Fig. 3D), and body mass normalised fibre length and PCSA (Fig. 3E). Therefore, these anatomically and functionally diverse examples of mammalian muscle provide a unique opportunity to examine the potential differences in eccentric muscle properties, should they exist. The isometric properties of these four muscles were significantly different in their twitch-rise time (ANOVA $F_{3,28}$=209.256, P<0.001, Table 1) and half-relaxation time (ANOVA $F_{3,28}$=158.956, P<0.001, Table 1). Moreover, the muscle shortening force-velocity properties of these four muscles were significantly different (Table 1) with significantly different maximum shortening velocities (ANOVA $F_{3,28}$=35.306, P<0.001, Fig. 4A, D, G, J, Table 1), $\dot{W}_{max}$ (ANOVA $F_{3,28}$=35.101, P<0.001, Fig. 4A, D, G, J, Table 1) and power ratios (ANOVA $F_{3,28}$=16.623, P<0.001, Fig. 4A, D, G, J, Table 1).

In addition to the distinct muscle shortening properties, there were significant differences in the eccentric plateau height coefficient (ANOVA $F_{3,27}$=24.462, P<0.001, Fig. 4A, D, G, J, Table 2) and curvature coefficient (ANOVA $F_{3,27}$=3.481, P=0.029, Fig. 4A, D, G, J, Table 2) across the four muscles. As found in the mouse SOL and EDL, the rat DIA (Fig. 4G-I) and the rabbit DIG (Fig, 4J-L) muscle also exhibited a significantly strong correlation between the rate of change of relative force with respect to time and stretch velocity during both phase-1 (DIA r_{rm} (39) = -0.9837, 95% CI [-0.9913, -0.9694], p<0.001; DIG r_{rm} (11) = -0.9567, 95% CI [-0.9873, -0.8578], p<0.001) and phase-2 (DIA r_{rm} (39) = -0.9781, 95% CI [-0.9884, -0.9591], p<0.001; DIG DIG r_{rm} (11) = -0.9471, 95% CI [-0.9844, -0.8284], p<0.001), respectively. Moreover, pooling data from all four muscles shows that there is a significantly conserved absolute fibre lengthening velocity-dependant relationship with the rate of force development across the two phases of mammalian muscle (Fig. 5A, phase-1 r_{rm} (114) = -0.9663, 95% CI [-0.9765, -0.9516], p<0.001; Phase-2 r_{rm} (114) = -0.9167, 95% CI [-0.9417, -0.8818], p<0.001) and normalised fibre lengthening velocity (phase-1 r_{rm} (114) = -0.9631, 95% CI [-0.9744, -0.9471], p<0.001; phase-2 r_{rm} (114) = -0.9147, 95% CI [-0.9402, -0.8790], p<0.001, Fig. 5B). As well as the significantly conserved phase-1 and phase-2 rates of

force development in relation to stretch velocity, the transition point between the two phases is significantly correlated with lengthening velocity across all four muscles (Fig. 6A-D) and the pooled muscle data (Fig. 6E-F), occurring at a higher P/P_0 with increasing velocity of stretch. Finally, the relationship between rate of force development and stretch velocity is robust regardless of force normalisation strategy, including normalisation to PCSA (Appendix Fig. 4, phase-1 r_{rm} (114) = -0.9667, 95% CI [-0.9769, -0.9522], p<0.001; phase-2 r_{rm} (114) = -0.9079, 95% CI [-0.9354, -0.8695], p<0.001), which may be of more translatable benefit to Hill-type musculoskeletal modellers (Rajagopal *et al.*, 2016; Charles *et al.*, 2022; Kissane *et al.*, 2022).

The dynamic two-phase eccentric contraction response is not a function of passive muscle properties, but is dependent on titin activation.

The passive muscle properties across all four muscles tested differed in relation to the active length-force relationship (Fig. 7A-D, F). The passive force at L_0 as a proportion of isometric twitch force was significantly different between the four muscles, ranging from 0.34 in SOL to 0.05 in DIG (ANOVA $F_{3,23}$=11.724, P<0.001, Fig. 7E). To examine the contribution of the passive muscle properties to the eccentric force-velocity relationship we performed active and passive eccentric ramps in the SOL, EDL and DIG (Fig. 8, Appendix Fig. 5). We show that despite significantly different passive muscle properties (Fig. 7) it appears to have no significant contribution to the force profiles during lengthening of the DIG (Appendix Fig. 5), SOL (Fig. 8) or EDL (Fig. 8) muscles. Briefly, individual active and active-minus-passive traces (Appendix Fig. 5A-C) highlight the lack of contribution to the overall eccentric force profile and bear no significant contribution to the eccentric force-velocity relationship (Appendix Fig. 5G). Despite the significantly different passive force at L_0 between the mouse SOL and EDL (Fig. 7E) there was no significant effect of these properties on the eccentric force-velocity relationship when accounting for passive force (Fig. 8A). While the SOL and EDL have significantly different D (-0.287 ± 0.056 *vs.* -0.522 ± 0.031, P<0.001, Fig. 8B, Table 2) and E coefficients (0.265 ± 0.105 *vs.* 0.537 ± 0.135, P=0.005 Fig. 8C, Table 2), when accounting for the passive force (i.e. active force minus passive force) there was no significant change in the coefficient values in either muscle (Fig. 8A-C). Consequently there was no significant difference in the regression slopes for the relationship between rate force development and velocity of stretch in SOL (t(59)=1.6765, P=0.099, Fig. 8D) or EDL (t(48)=1.5889, P=0.119, Fig. 8E) when accounting for the passive force properties of the muscles.

Mice with impaired titin activation still have a relatively typical two-phase response to eccentric loading (Fig. 9A) and present with a significant relationship between the lengthening velocity and

the rate of force development (Fig. 9B-C). The rate of force development during the first phase of the eccentric ramp was not significantly different between the wild type (wt) and mdm mice ($t(41)=0.9057$, $P=0.3704$, Fig. 9B), and was not significantly different when accounting for passive muscle properties ($t(41)=1.1491$, $P=0.2572$, Fig. 9D). However, the second phase in the mdm muscle presents with a comparable significant relationship between the rate of force development and velocity of stretch (Fig. 9C), yet when accounting for the contribution of the passive muscle properties this relationship is completely abolished (Fig. 9E). These data highlight the importance of titin activation on the rate of force development during eccentric muscle contractions.

Discussion

Despite the eccentric force-velocity relationship being generally described over eighty years ago, little progress has been made in determining whether muscle anatomical or intrinsic contractile properties underpin the shape of this relationship. This uncertainty presents a problem for modelling muscle behaviours that involve eccentric contractions, which is a common feature of many muscles that function during cyclical behaviours like locomotion (Askew & Marsh, 2001; Gillis & Biewener, 2001; Gillis *et al.*, 2005; Roberts *et al.*, 2007; Mayerl *et al.*, 2021). Here we present a comprehensive and robust data set of the complete (both concentric and eccentric) force-velocity relationships from mammalian muscles differing in both phenotype and muscle mass. We have shown that there are significant differences in the plateau height of the eccentric force-velocity relationship across this range of mammalian muscles. However, the more robust relationship may be that describing the rate of relative force development during eccentric muscle activation, the relationship being highly conserved. Finally, we show that the rate of relative force development during phase-2 of eccentric force-development is dependent on normal titin activation, while the initial first phase is not.

The inherent difficulty in characterising the eccentric force-velocity relationship.

In previous investigations there has been a lack of consistency in the experimental protocol used to study the eccentric force-velocity relationship. This has made it difficult to identify and characterise the eccentric muscle properties, which is required to develop reliable musculoskeletal models of muscle dynamic behaviours (Rajagopal *et al.*, 2016). Many previous studies have completed eccentric ramps on the ascending limb of the force-length relationship (Krylow & Sandercock, 1997), while others have been conducted at non-physiological temperatures (Lännergren, 1978; Edman, 1988; Lombardi & Piazzesi, 1990; Alcazar *et al.*, 2019), factors which are all thought to influence the eccentric force-velocity response (Alcazar *et al.*, 2019). The lack of comprehensive data and standardised methodological approach has meant that approaches for modelling the eccentric force-velocity relationship in computational Hill-type musculoskeletal models have depended on narrow, and arguably inappropriate sets of experimental data. For example, Millard et al. (2013) (Millard *et al.*, 2013) modelled the eccentric force-velocity relationship using data from an *in-situ* preparation of the cat soleus muscle (Joyce *et al.*, 1969) (at 37 °C) and the *ex-vivo* force-velocity relationship from the semitendinosus muscle of the frog (at 10 ºC) (Mashima *et al.*, 1972).

Additionally, there has been no standardisation of the relative length on the force-length relationship that has been used to derive force for normalising the eccentric force-velocity relationship. This is problematic, given the biphasic force development response to stretch, since it is possible to produce dramatically different eccentric force-velocity relationships when taking just a single point value to define this relationship. While measuring the differential of relative force across phase-1 or phase-2 would yield a similar value regardless of measurement site as the two responses are virtually linear, and thus, less prone to error. We have demonstrated this to be a more reliable descriptor of the dynamic eccentric force-velocity relationship.

Mechanistic underpinning of the eccentric biphasic force development response.

It has long been established that shortening force-velocity properties differ between muscles that are predominantly fast- or slow contracting (Askew & Marsh, 1997), yet conflicting data exist on the eccentric force-velocity properties between fast- and slow-muscles, with some studies reporting no difference (Rijkelijkhuizen *et al.*, 2003) and others reporting subtle velocity-specific differences (Stienen *et al.*, 1992; Ramsey *et al.*, 2010). Our data show that mouse SOL and EDL have significantly distinct muscle properties in terms of both the concentric and eccentric force-velocity relationships, with the SOL attaining a greater plateau height and more curved force-velocity profile compared to EDL during the eccentric force-velocity relationship. This observation appear to be consistent with those of Linari *et al.* (2004) who showed slow twitch fibres from humans to have a greater plateau height compared to fast twitch fibres. However, when comparing the rate of relative force development, both muscles appear to have similar profiles across normalised velocities. This is in contrast to findings of muscles eccentrically stretched during cyclical contractions (Hessel & Nishikawa, 2017) however, the rate of change of force presented in our work here has been normalised to peak isometric force, whereas in Hessel and Nishikawa (2017), absolute forces were compared. Our findings here are further complicated when we consider the DIA and DIG which have a mixed fibre type composition. Both the DIA and DIG have a greater plateau height compared to that of the slow SOL, which suggests that this parameter is not underpinned by fibre phenotype. It is possible that the different relative stretch amplitude across our mammalian muscles may be masking subtle differences in muscle fibre phenotype (Krylow & Sandercock, 1997; Josephson & Stokes, 1999), and as such requires further exploration.

The physiological underpinning of the distinct biphasic force development response during eccentric lengthening is still a contentious topic. It is thought that the initial rapid phase-1 profile is a response to elevated strain of attached cross-bridges, after which the detachment of myosin heads

leads to the transition into a shallower phase-2 force response (Tomalka *et al.*, 2020, 2021; Weidner *et al.*, 2022; Tomalka, 2023). While the phase-2 force response is thought to be linked to increased strain of non-crossbridge parallel elastic elements (Ramsey *et al.*, 2010; Tomalka, 2023). To the best of our knowledge this is the first comprehensive overview of eccentric muscle characteristics in mammalian muscle. We have shown for the first time that the initial phase-1 response (i.e. crossbridge activation) is velocity-dependent, and this relationship is conserved over 3 orders of magnitude of mammalian skeletal muscle mass. This may be indicative of a comparable proportion of cross-bridges are attached during the steep force rising phase-1. Additionally, we show that this rapid force development phase-1 response is neither affected by passive muscle properties, nor activation of titin, providing further support to the hypothesis that this is predominantly driven by cross-bridge activation. Interestingly, previous work on the dependence of the transition point between phase-1 and -2 has been inconclusive in establishing a relationship, with frog/toad muscles presenting with a biphasic velocity dependent response that plateaus at ~1.5 P/P_0, while the mouse soleus presented with a curvilinear velocity dependence (Stienen *et al.*, 1992). We show here that across our four mammalian muscles there are significant linear relationships between the transition point and lengthening velocity.

Phase-2 of the force development profile has been equally under-investigated, despite it being routinely described in the literature (Joyce *et al.*, 1969; Lombardi & Piazzesi, 1990; Stienen *et al.*, 1992; Josephson & Stokes, 1999; Tomalka, 2023). Again, this is likely in-part due to the lack of standardised experimental approaches for muscle lengthening experimentation and quantification. Our data shows there to be a significant relationship with the rate of force development and velocity of muscle lengthening for phase-2 of the force development response. This response does not appear to be affected by passive muscle properties, but is reliant on normal titin activation. The SOL and EDL express different titin isoforms (Hettige *et al.*, 2022), which have been proposed to affect passive forces differentially (Prado *et al.*, 2005), yet they presented with comparable rates of force development across phase-2 of the eccentric ramp. There are several possible reasons, firstly it may be that different titin isoforms do not play a role in the rate of force development during stretch but are integral to the level of force enhancement following cessation of stretch. Alternatively, this may suggest that additional, non-contractile elements contribute to this force enhancement (Prado *et al.*, 2005; Hettige *et al.*, 2020; Hettige *et al.*, 2022).

Our data provide a novel insight into the dynamic force enhancement response to muscle stretch. In the first instance our collective mammalian data suggest that the current default Hill-type musculoskeletal model of the eccentric force-velocity relationship which plateaus at 1.40 P/P_0

(Millard *et al.*, 2013), is actually underestimating the plateau by 18% (our average mammalian plateau occurs at 1.65 P/P_0). Additionally, the current representation of the eccentric force-velocity as a hyperbolic fit may be too simplistic given the dynamic biphasic response of muscle force to stretch and therefore, musculoskeletal models should incorporate the rate of force development. The data presented here enable the calculation of the transition between the rapid force development of phase-1 and the shallower phase-2. These data may provide a foundational step towards improving Hill type musculoskeletal model predictions; however this relationship has only been validated in maximally activated muscles, and this relationship may not represent the true eccentric biphasic response under normal physiological recruitment.

Experimental limitations

The lack of consistency in the experimental protocols that have been used to study the eccentric force-velocity relationship makes it inherently difficult to critically compare data between studies. For example, many previous studies have conducted eccentric ramps at different positions (relative to L_0) on the force-length relationship with some studies performing contractions entirely on the ascending limb and never crossing L_0 (Krylow & Sandercock, 1997), while others have used lengthening contractions that occur symmetrically across L_0 (Tahir *et al.*, 2020) but have varied strain. While we have consistently subjected our four mammalian muscles to symmetrical length excursions across L_0 for each of these muscles, the relative strain each muscle was subjected to was not equal, and as such the variability presented here may be in part a consequence of this. Rat muscles stretched at the same velocity at different positions on the ascending limb of the force-length relationship show a shift in the transition point between the phase-1 and phase-2 force profiles (Krylow & Sandercock, 1997) as well as the plateau of the eccentric side of the force-velocity relationship. However, it should be noted that these data were presented as absolute force, in contrast to the data we report, which has been normalised to P_0, the impact of which is currently unknown. There is an inherent difficulty in generating a standardised approach to assess the eccentric force-velocity relationship in whole muscle preparations. Simply using a constant strain across L_0 (e.g. ±10% L_0) could be argued inappropriate. Our data (Fig. 8) highlight the significant difference in the force-length relationships across mammalian muscle (Mendoza *et al.*, 2023), with for example a ± 10% L_0 strain on the DIG muscle would descend down the ascending/descending limb to as low as 60% of P_0 while the same strain in the DIA would not drop below 80% of P_0. More work is required to comprehensively characterise the importance of position on the force-length relationship on the eccentric behaviour of muscle (Krylow & Sandercock, 1997; Tomalka *et al.*, 2017). Further, complications arise when considering the method with which eccentric muscle properties are derived, as previously noted differences may

exist in the force-velocity profiles when derived from isovelocity or from isotonic experimentation (Woledge *et al.*, 1985). While our data here are derived from isovelocity experiments like those used to develop default OpenSim parameters (Millard *et al.*, 2013) the sensitivity of these models to data derived from isovelocity and isotonic approaches are unknown. This poses compelling consideration for incorporation of these data into Hill type musculoskeletal models, and highlights many avenues for future work.

In conclusion, our standardised approach has shown there to be a conserved relationship between the velocity of muscle lengthening and the rate of force development across mammalian muscle. The characterisation of the rate of force development of the biphasic force response may be a more reliable way to describe the forces during eccentric muscle contractions compared to the traditional hyperbolic curve fitting. Our data support the hypothesis that the rapid force (phase-1) development during muscle lengthening is a function of crossbridge activation while the slower phase of force development (phase-2) is reliant on titin activation.

Author Contribution

Conceptualisation, R.W.P.K and G.N.A.; Methodology, R.W.P.K and G.N.A.; Formal Analysis, R.W.P.K; Writing – Original Draft, R.W.P.K; Writing – Reviewing & Editing, G.N.A.; Funding Acquisition, R.W.P.K and G.N.A.

Data Availability

Data is available at the University of Liverpool's Data Repository (https://datacat.liverpool.ac.uk/id/eprint/2427)

Declaration of Interests

The authors declare no competing interests.

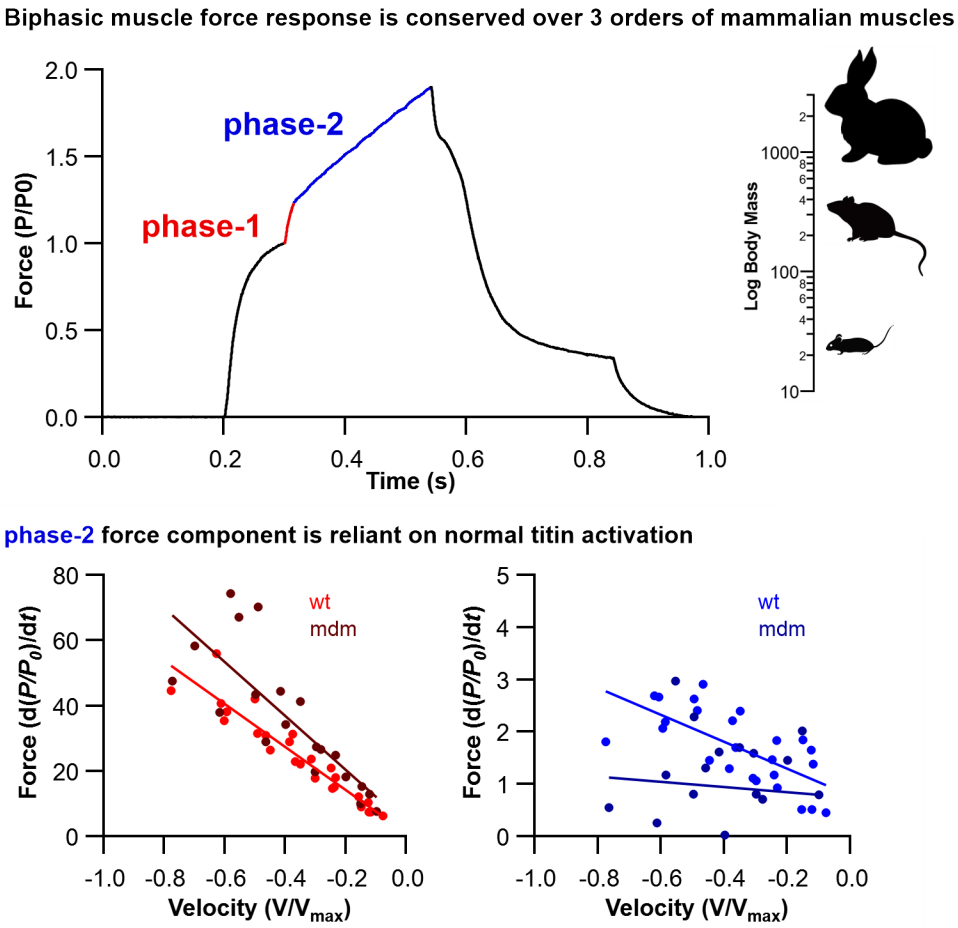

492

493 **Abstract Figure Legend.** Here we have shown that the biphasic force response seen during active
494 muscle lengthening is conserved over three orders of magnitude of mammalian skeletal muscle mass.
495 Using mice with a small deletion in titin (mdm) we show that the phase-2 portion (blue) of the
496 biphasic force profile in response to muscle lengthening is reliant on normal titin activation. The rate
497 of force development during muscle stretch may be a more reliable way to describe the forces
498 experienced during eccentric muscle contractions compared to the traditional hyperbolic curve fitting,
499 and functions as a novel predictor of force-velocity characteristics that may be used to better inform
500 musculoskeletal models and assess pathophysiological remodelling.

501

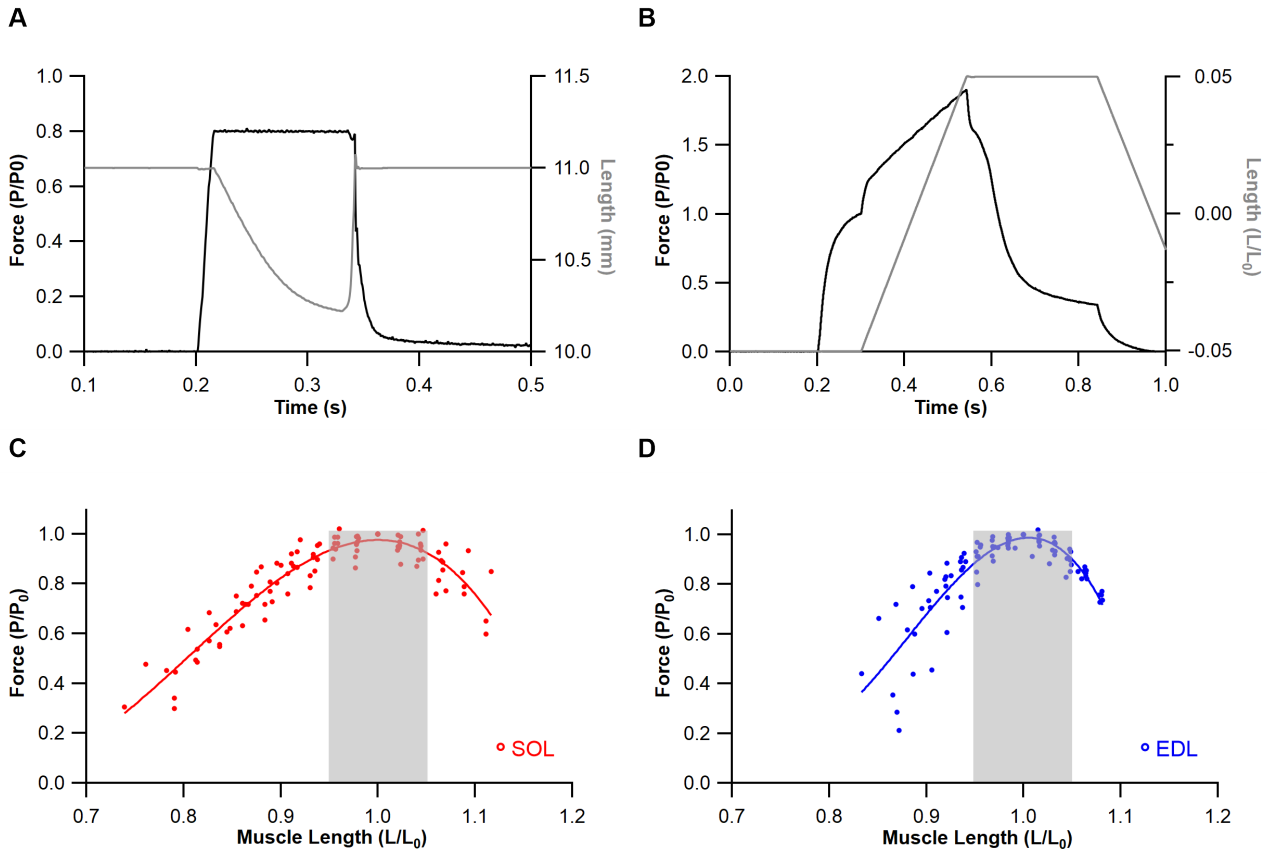

Figure 1. Muscle mechanical procedure. Isotonic muscle shortening (A) and isovelocity muscle lengthening (B) protocols. Complete force-length relationships for the soleus (C) and extensor digitorum longus (D) with the shaded region highlighting the region with which isovelocity lengthening was conducted.

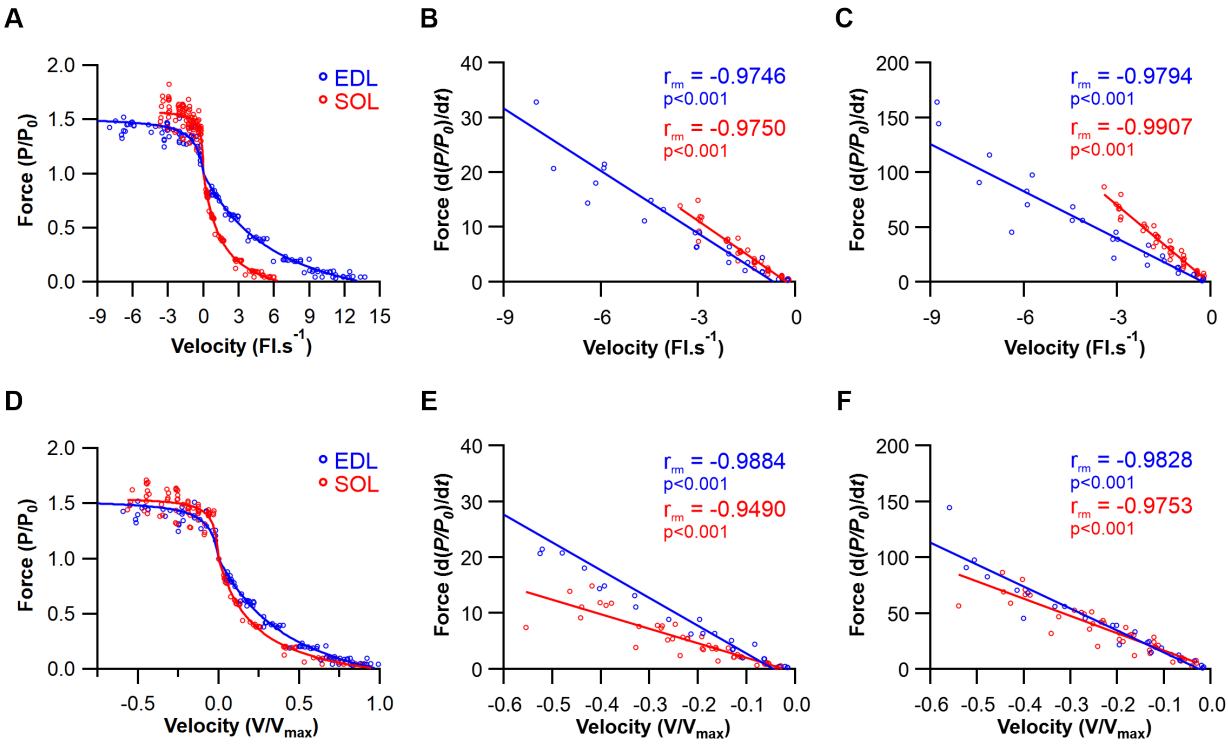

Figure 2. Muscle force-velocity characteristics of two phenotypically distinct muscles. Absolute force velocity relationship (A). Rate of force development as a function of lengthening velocity across the phase-2 (B) and phase-1 (C). Normalised force velocity relationship (D). Rate of force development as a function of normalised lengthening velocity across the phase-2 (E) and phase-1 (F).

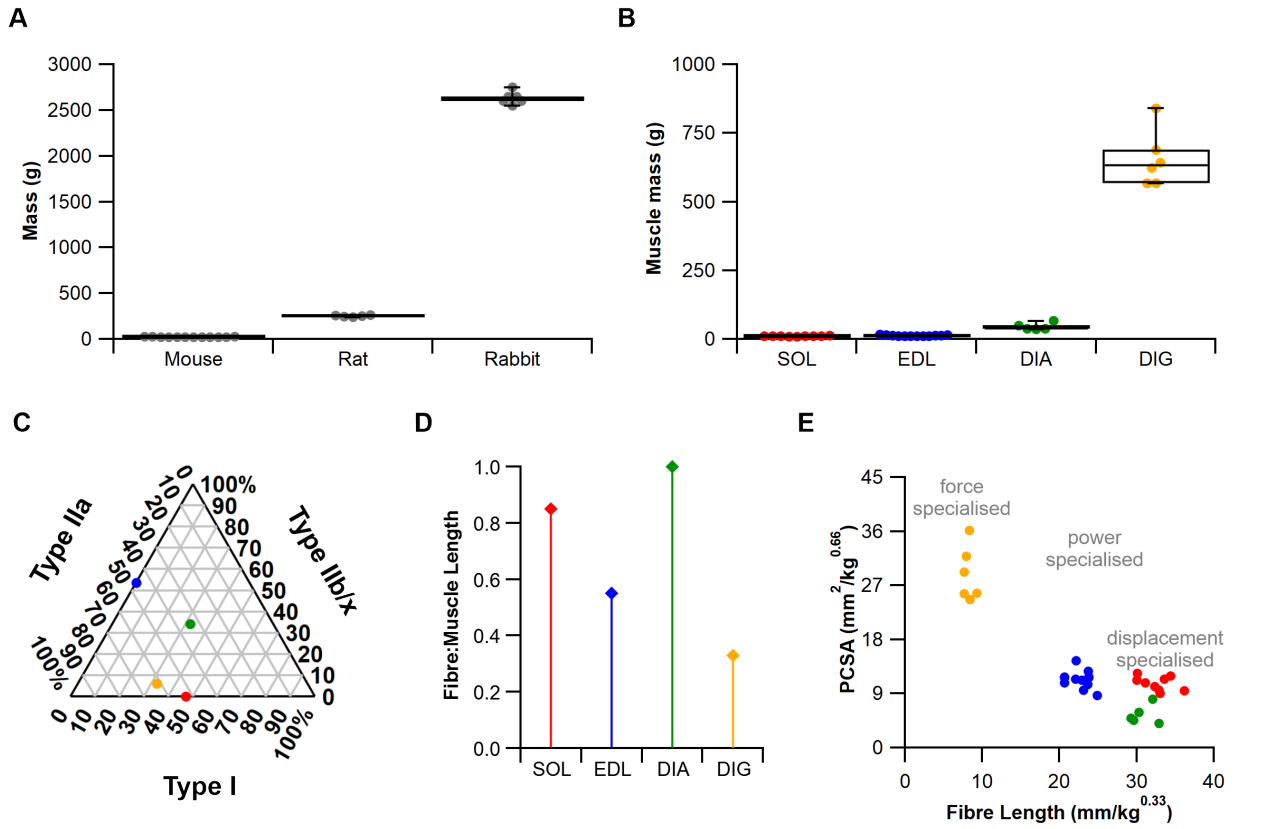

Figure 3. Comparative muscle architecture across mammalian muscles. Here we have used species that range three order of magnitude in body mass (A) and muscle mass (B). These muscles have distinctive muscle fibre phenotypes (C), relative muscle fibre to whole muscle lengths (D) and are architecturally distinct in their muscle morphology (E).

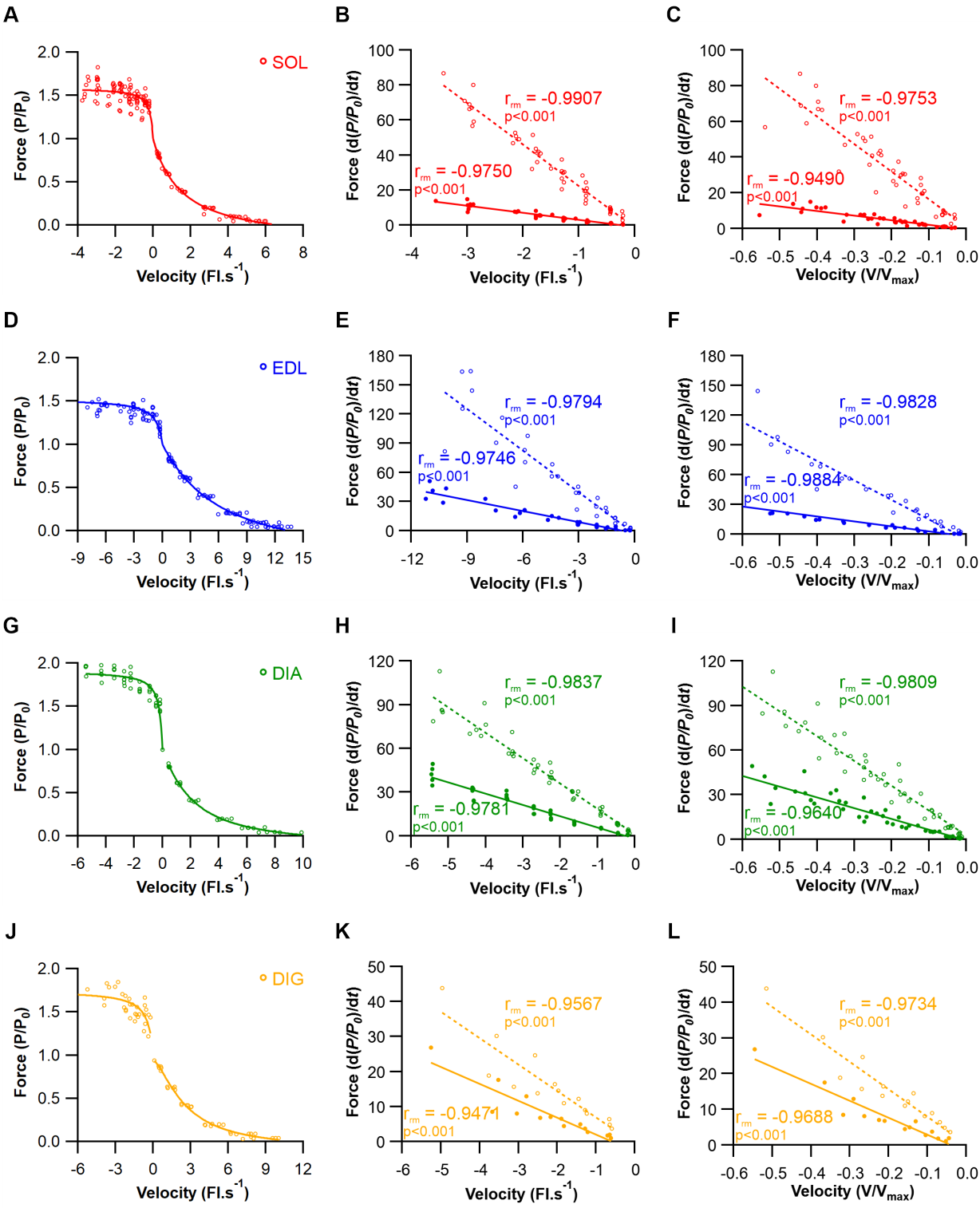

Figure 4. Force-velocity characteristics across four mammalian muscles. Absolute force velocity relationship (A, D, G, J), rate of force development as a function of absolute lengthening velocity across the first phase (dashed line) and second phase (solid line) of the isovelocity relationship (B, E, H, K). Rate of force development as a function of normalised lengthening velocity across the first phase (dashed line) and second phase (solid line) of the isovelocity relationship (C, F, I, L). Presented

for the mouse soleus (A, B, C), mouse extensor digitorum longus (D, E, F), rat diaphragm (G, H, I) and rabbit digastric (J, K, L) muscles.

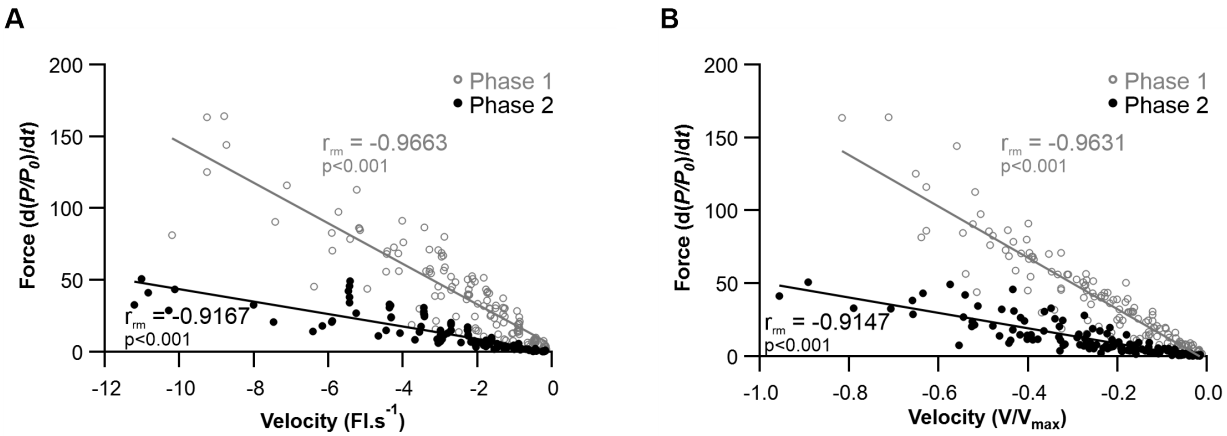

529

530 **Figure 5. Pooled rate of force development as a function of P_0 during eccentric contractions.**
531 Pooled rate of force development as a function of absolute (fibre lengths per second) lengthening
532 velocity (A) and normalised lengthening velocity (to maximum shortening velocity, V_{max}) (B) across
533 phase-1 (unfilled grey) and phase-2 (filled black) (B) of the isovelocity lengthening relationship.

534

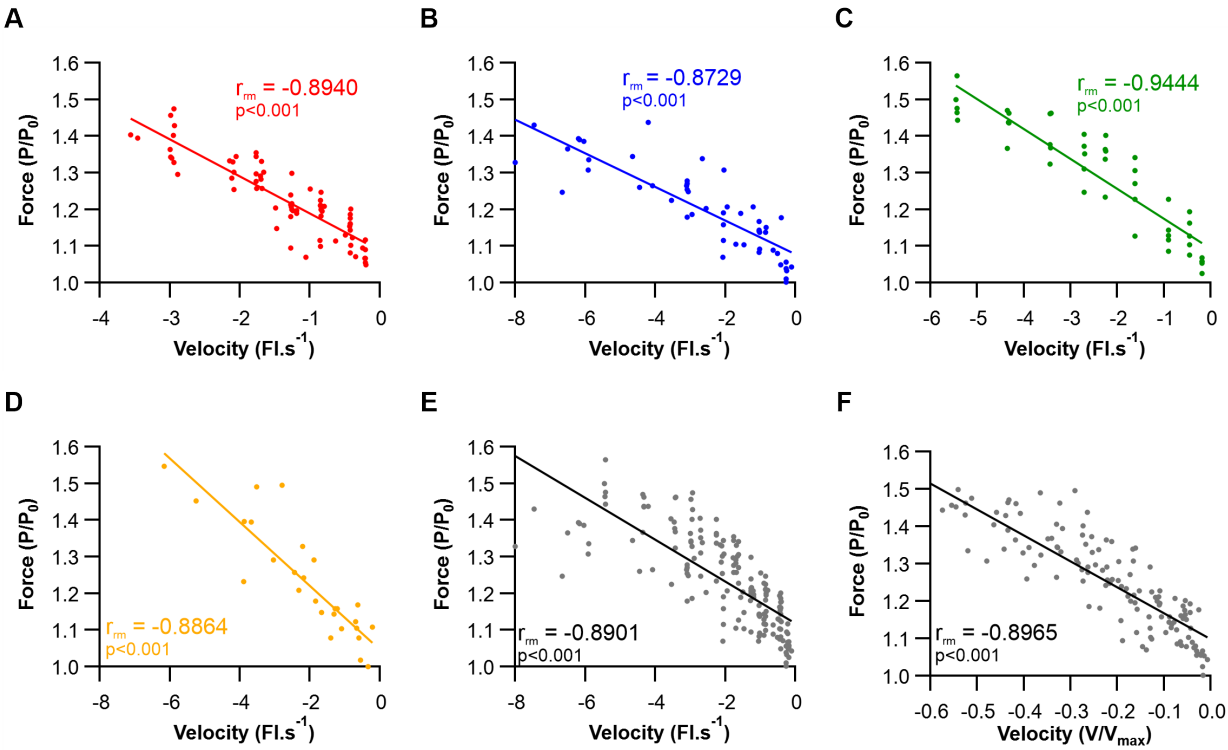

535

536 **Figure 6. Relationship between the transition point between phase-1 and phase-2 of force**
537 **development and lengthening velocity during the eccentric force-velocity relationship.** The
538 relationship between lengthening velocity and the transition from phase-1 to phase-2 for the SOL (A),
539 EDL (B), DIA (C) and DIG (D) show significantly strong positive relationships. When pooled for
540 absolute lengthening velocity (E) and normalised to V_{max} (F) this significant relationship is
541 maintained.

542

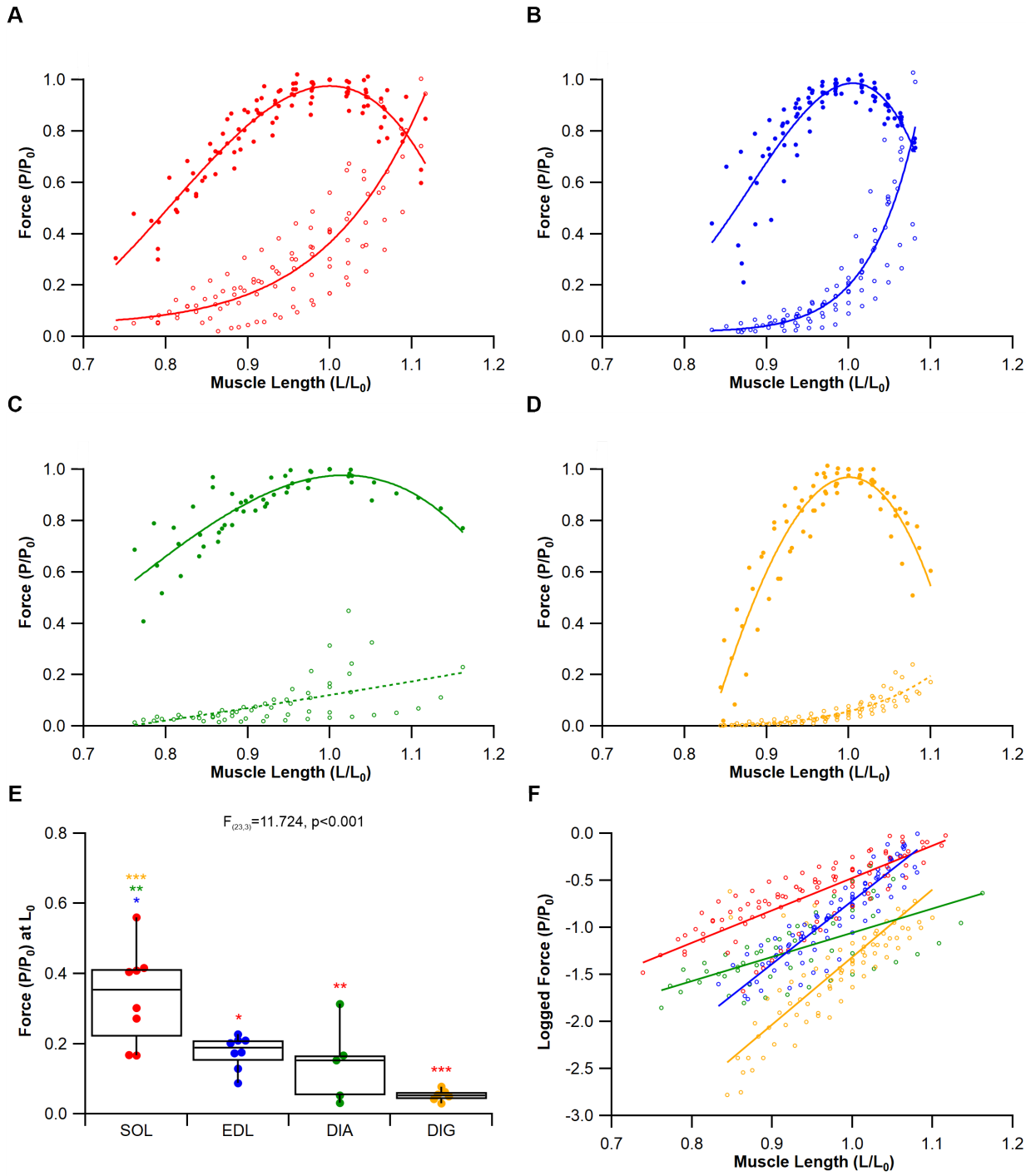

Figure 7. Active and passive muscle force-length relationship in different mammalian muscles. Force-length relationship for the soleus (A), extensor digitorum longus (B), diaphragm (C) and digastric (D) muscles for active (solid filled circles) and passive muscles (unfilled circles). Having analysed the eccentric force-velocity behaviour at L_0 we present the relative passive force at L_0 (E) highlighting the difference in passive muscle properties across the four muscles. Finally, the logged relative passive forces across the force-length relationship (F), further emphasising the differences in rate of passive force development. * P<0.05, **P<0.01, ***P<0.001.

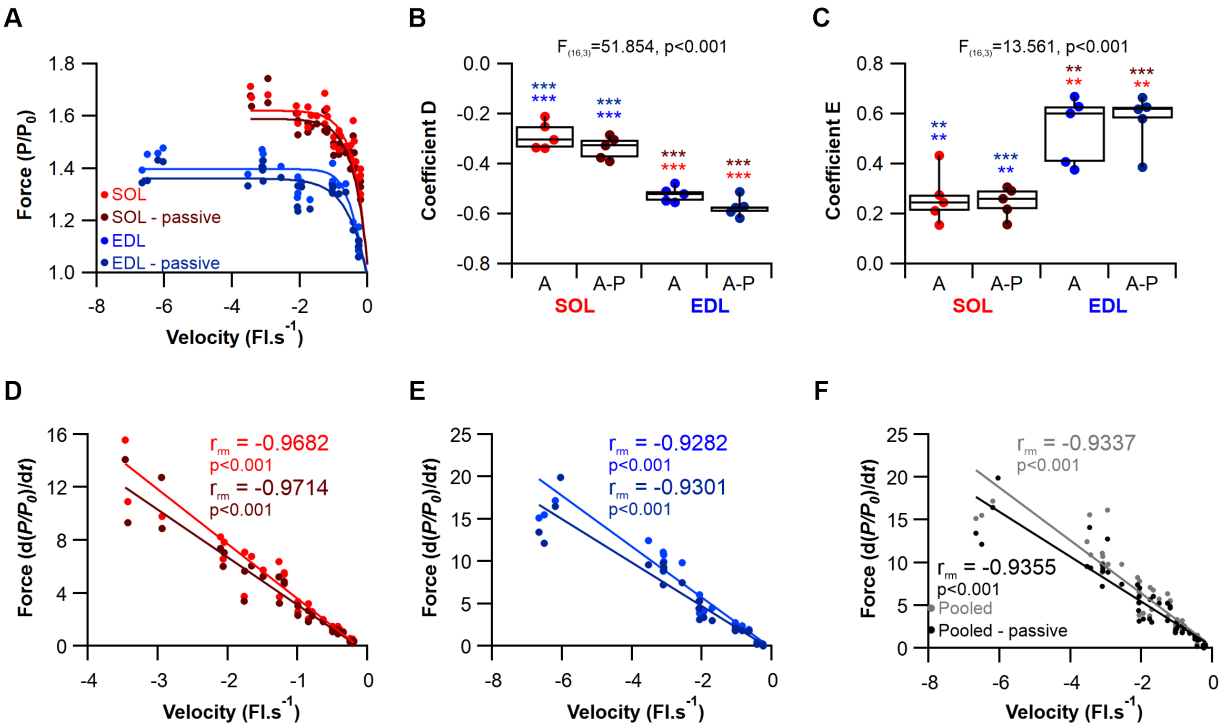

551

552 **Figure 8. Effect of passive muscle properties during muscle lengthening of the mouse soleus and**
553 **extensor digitorum longus muscles.** Eccentric force-velocity relationship for the SOL and EDL for
554 the active data, and the active data minus passive eccentric ramps (A). There is a significant difference
555 between the SOL and EDL coefficient D, but not between active *vs.* active minus passive force-
556 velocity profiles (B). Similarly, there is a significant difference between coefficient E of the SOL and
557 the EDL, but no difference when accounting for passive force contribution during eccentric ramps
558 (C). The relationship between $dx/dt/P_0$ remains significantly correlated with velocity for the SOL (D)
559 and EDL (E), however there is no effect when amending for passive force during the eccentric ramp.
560 Finally, the pooled relationship between $dx/dt/P_0$ and lengthening velocity remains significantly
561 correlated with velocity (F). * P<0.05, **P<0.01, ***P<0.001.

562

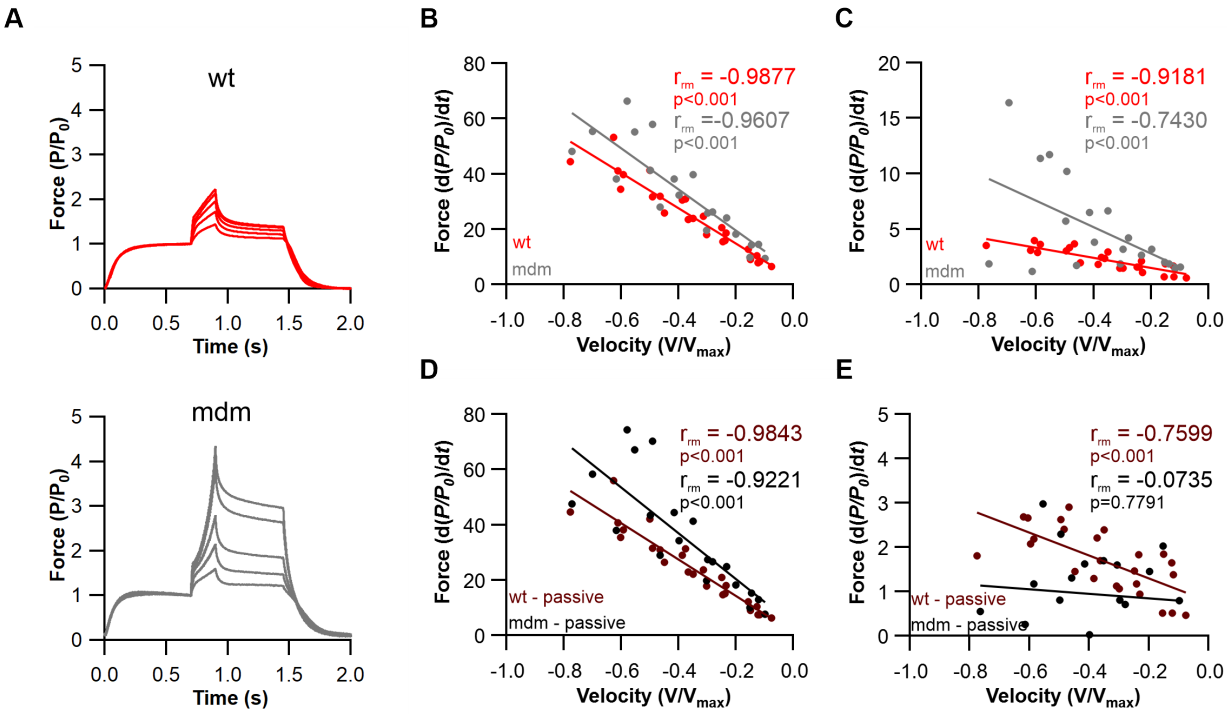

Figure 9. Contribution of titin to the eccentric force-velocity relationship in mouse soleus muscle. Eccentric ramps during tetanic contractions for wild type (wt) and titin knock out (mdm) soleus muscle (A). The rate of force development as a function of normalised lengthening velocity across phase-1 (B, D) and phase-2 (C, E) on absolute force (B, C) and when accounting for passive force (D, E).

Table 1. Isometric and isotonic properties of the soleus (SOL), extensor digitorum longus (EDL), diaphragm (DIA) and digastric (DIG) muscle.

	SOL	EDL	DIA	DIG	F	P value
Isometric stress (kN.M^{-2})	203.2 ± 46 †	236.4 ± 51.1†	185.3 ± 16.0†	383.7 ± 76.6 * § #	18.39	<0.001
Twitch rise time (ms)	17.2 ± 1.8 § † #	8.0 ± 0.6 * † #	22.3 ± 2.1* § †	36.5 ± 4.4 * § #	209.256	<0.001
Half relaxation time (ms)	21.3 ± 2.4 § † #	9.4 ± 1.8 * † #	26.3 ± 1.9 * § †	30.4 ± 2.4 * § #	158.956	<0.001
V_{max}	7.01 ± 0.6 § † #	14.14 ± 1.77 *† #	10.18 ± 1.58 * §	11.09 ± 2.13 * §	35.306	<0.001
$\dot{W}_{max}$	120.0 ± 32.6 §	402.6 ± 108.2*	160.8 ± 23.3§	142.4 ± 29.6 §	35.101	<0.001
P/P_0 at maximal power	0.30 ± 0.02 §	0.39 ± 0.02*	0.33 ± 0.01 § †	0.38 ± 0.05 * #	20.505	<0.001
V/V_{max} at maximum power	2.05 ± 0.19 § † #	4.64 ± 0.63* † #	2.81 ± 0.25* § †	0.98 ± 0.13 * § #	121.536	<0.001
Power ratio	0.089 ± 0.008 §	0.128 ± 0.013* † #	0.091 ± 0.006 §	0.104 ± 0.023 §	16.623	<0.001
V/V_{max}	2.05 ± 0.19	3.08 ± 0.46	3.61 ± 0.25	3.47 ± 0.34	2.852	0.055

V_{max}; maximum shortening velocity, W_{max}; maximum isotonic power. Mean value ± standard deviation. * P<0.05 *vs.* SOL, § P<0.05 *vs.* EDL, # P<0.05 *vs.* DIA, † P<0.05 *vs.* DIG.

571

Table 2. Coefficients for the force-velocity relationship fit to the soleus (SOL), extensor digitorum longus (EDL), diaphragm (DIA) and digastric (DIG) muscle.

	SOL	**EDL**	**DIA**	**DIG**	**F**	**P value**
A	0.244 ± 0.130	0.396 ± 0.295	0.190 ± 0.036	0.172 ± 0.069	2.355	0.093
B	1.81 ± 1.18	5.56 ± 5.39 †	1.75 ± 0.13	0.511 ± 0.258 §	3.843	0.020
C	-0.157 ± 1.045	1.547 ± 3.019	0.779 ± 0.377	0.657 ± 0.358	1.276	0.302
D	-0.313 ± 0.063 § #	-0.500 ± 0.039 * † #	-0.0872 ± 0.0485 * §	-0.190 ± 0.216 §	24.462	<0.001
E	0.289 ± 0.117 †	0.571 ± 0.313	0.231 ± 0.051	0.960 ± 1.000 *	3.481	0.029

Coefficient A, B and C correspond to values for the Marsh and Bennett (1986) hyperbolic linear equation fit for the concentric portion of the force-velocity relationship presented in Equation 1. While D and E correspond to value fit for the rearranged hyperbolic equation from Alcazar, et al. (2019) to fit the eccentric portion of the force-velocity relationship, displayed in Equation 2. Mean value ± standard deviation. * P<0.05 *vs.* SOL, § P<0.05 *vs.* EDL, # P<0.05 *vs.* DIA, † P<0.05 *vs.* DIG.

572

573 # References

574 Alcazar J, Csapo R, Ara I & Alegre LM. (2019). On the shape of the force-velocity relationship in
575 skeletal muscles: The linear, the hyperbolic, and the double-hyperbolic. *Frontiers in*
576 *Physiology* **10,** 769.

577

578 Altringham JD & Young IS. (1991). Power output and the frequency of oscillatory work in
579 mammalian diaphragm muscle: the effects of animal size. *Journal of Experimental*
580 *Biology* **157,** 381-389.

581

582 Askew GN. (2023). Adaptations for extremely high muscular power output: why do muscles
583 that operate at intermediate cycle frequencies generate the highest powers? *Journal of*
584 *Muscle Research and Cell Motility*.

585

586 Askew GN & Marsh RL. (1997). The effects of length trajectory on the mechanical power output
587 of mouse skeletal muscles. *Journal of Experimental Biology* **200,** 3119-3131.

588

589 Askew GN & Marsh RL. (2001). The mechanical power output of the pectoralis muscle of blue-
590 breasted quail (Coturnix chinensis): the in vivo length cycle and its implications for
591 muscle performance. *Journal of Experimental Biology* **204,** 3587-3600.

592

593 Askew GN, Young IS & Altringham JD. (1997). Fatigue of mouse soleus muscle, using the work
594 loop technique. *Journal of Experimental Biology* **200,** 2907-2912.

595

596 Azizi E. (2014). Locomotor function shapes the passive mechanical properties and operating
597 lengths of muscle. *Proceedings of the Royal Society B: Biological Sciences* **281,** 20132914.

598

599 Bakdash JZ & Marusich LR. (2017). Repeated Measures Correlation. *Frontiers in Psychology* **8**.

600

601 Barclay C. (1996). Mechanical efficiency and fatigue of fast and slow muscles of the mouse. *The*
602 *Journal of Physiology* **497,** 781-794.

603

604 Blum KP, Campbell KS, Horslen BC, Nardelli P, Housley SN, Cope TC & Ting LH. (2020). Diverse
605 and complex muscle spindle afferent firing properties emerge from multiscale muscle
606 mechanics. *Elife* **9,** e55177.

607

608 Blum KP, Lamotte D'Incamps B, Zytnicki D & Ting LH. (2017). Force encoding in muscle spindles
609 during stretch of passive muscle. *PLoS Computational Biology* **13,** e1005767.

610

611 Burton RF. (1975). *Ringer solutions and physiological salines*. Wright-Scientechnica.

612

613 Charles J, Kissane R, Hoehfurtner T & Bates KT. (2022). From fibre to function: are we
614 accurately representing muscle architecture and performance? *Biological Reviews* **97,**
615 1640-1676.

616

617 Dantuma R & Weijs W. (1980). Functional anatomy of the masticatory apparatus in the rabbit
618 (Oryctolagus cuniculus L.). *Netherlands Journal of Zoology* **31,** 99-147.

619

620 De Ruiter C, Didden W, Jones D & De Haan A. (2000). The force-velocity relationship of human
621 adductor pollicis muscle during stretch and the effects of fatigue. *The Journal of*
622 *physiology* **526,** 671.

623

624 Edman K. (1988). Double ‐ hyperbolic force ‐ velocity relation in frog muscle fibres. *The*
625 *Journal of Physiology* **404,** 301-321.

626

627 Edman K, Elzinga G & Noble M. (1978). Enhancement of mechanical performance by stretch
628 during tetanic contractions of vertebrate skeletal muscle fibres. *The Journal of*
629 *Physiology* **281,** 139-155.

630

631 Espino ‐ Gonzalez E, Tickle PG, Benson AP, Kissane RW, Askew GN, Egginton S & Bowen TS.
632 (2021). Abnormal skeletal muscle blood flow, contractile mechanics and fibre
633 morphology in a rat model of obese ‐ HFpEF. *The Journal of Physiology* **599,** 981-1001.

634

635 Gillis GB & Biewener AA. (2001). Hindlimb muscle function in relation to speed and gait: in vivo
636 patterns of strain and activation in a hip and knee extensor of the rat (Rattus
637 norvegicus). *Journal of Experimental Biology* **204,** 2717-2731.

638

639 Gillis GB, Flynn JP, McGuigan P & Biewener AA. (2005). Patterns of strain and activation in the
640 thigh muscles of goats across gaits during level locomotion. *Journal of Experimental*
641 *Biology* **208,** 4599-4611.

642

643 Grundy D. (2015). Principles and standards for reporting animal experiments in The Journal of
644 Physiology and Experimental Physiology, pp. 755-758. Wiley Online Library.

645

646 Herzog W. (2014). The role of titin in eccentric muscle contraction. *Journal of Experimental*
647 *Biology* **217,** 2825-2833.

648

649 Herzog W, Schappacher G, DuVall M, Leonard TR & Herzog JA. (2016). Residual force
650 enhancement following eccentric contractions: a new mechanism involving titin.
651 *Physiology* **31,** 300-312.

652

653 Hessel AL & Nishikawa KC. (2017). Effects of a titin mutation on negative work during stretch–
654 shortening cycles in skeletal muscles. *Journal of Experimental Biology* **220,** 4177-4185.

655

656 Hettige P, Mishra D, Granzier H, Nishikawa K & Gage MJ. (2022). Contributions of titin and
657 collagen to passive stress in muscles from mdm mice with a small deletion in titin's
658 molecular spring. *International Journal of Molecular Sciences* **23,** 8858.

659

660 Hettige P, Tahir U, Nishikawa KC & Gage MJ. (2020). Comparative analysis of the transcriptomes
661 of EDL, psoas, and soleus muscles from mice. *BMC Genomics* **21,** 1-16.

662

663 Hill AV. (1938). The heat of shortening and the dynamic constants of muscle. *Proceedings of the*
664 *Royal Society of London Series B-Biological Sciences* **126,** 136-195.

665

Holt NC & Askew GN. (2012). The effects of asymmetric length trajectories on the initial mechanical efficiency of mouse soleus muscles. *The Journal of Experimental Biology* **215,** 324-330.

Josephson RK & Stokes DR. (1999). The force-velocity properties of a crustacean muscle during lengthening. *Journal of Experimental Biology* **202,** 593-607.

Joyce G, Rack P & Westbury D. (1969). The mechanical properties of cat soleus muscle during controlled lengthening and shortening movements. *The Journal of Physiology* **204,** 461-474.

Katz B. (1939). The relation between force and speed in muscular contraction. *The Journal of Physiology* **96,** 45.

Kissane RW, Charles JP, Banks RW & Bates KT. (2022). Skeletal muscle function underpins muscle spindle abundance. *Proceedings of the Royal Society B* **289,** 20220622.

Kissane RW, Charles JP, Banks RW & Bates KT. (2023). The association between muscle architecture and muscle spindle abundance. *Scientific Reports* **13,** 2830.

Kissane RWP, Egginton S & Askew GN. (2018). Regional variation in the mechanical properties and fibre-type composition of the rat extensor digitorum longus muscle. *Experimental Physiology* **103,** 111-124.

Kissane RWP, Wright O, Al'Joboori YD, Marczak P, Ichiyama RM & Egginton S. (2019). Effects of treadmill training on microvascular remodeling in the rat after spinal cord injury. *Muscle & Nerve* **59,** 370-379.

Krylow AM & Sandercock TG. (1997). Dynamic force responses of muscle involving eccentric contraction. *Journal of Biomechanics* **30,** 27-33.

Lai AK, Biewener AA & Wakeling JM. (2019). Muscle-specific indices to characterise the functional behaviour of human lower-limb muscles during locomotion. *Journal of Biomechanics* **89,** 134-138.

Lännergren J. (1978). The force—velocity relation of isolated twitch and slow muscle fibres of Xenopus laevis. *The Journal of Physiology* **283,** 501-521.

Linari M, Bottinelli R, Pellegrino MA, Reconditi M, Reggiani C & Lombardi V. (2004). The mechanism of the force response to stretch in human skinned muscle fibres with different myosin isoforms. *The Journal of Physiology* **554,** 335-352.

Lombardi V & Piazzesi G. (1990). The contractile response during steady lengthening of stimulated frog muscle fibres. *The Journal of Physiology* **431,** 141-171.

Luff A. (1981). Dynamic properties of the inferior rectus, extensor digitorum longus, diaphragm and soleus muscles of the mouse. *The Journal of Physiology* **313,** 161.

Marsh RL & Bennett A. (1986). Thermal dependence of contractile properties of skeletal muscle from the lizard Sceloporus occidentalis with comments on methods for fitting and comparing force-velocity curves. *Journal of Experimental Biology* **126,** 63-77.

Mashima H, AKAZAWA K, KUSHIMA H & FUJII K. (1972). The force-load-velocity relation and the viscous-like force in the frog skeletal muscle. *The Japanese Journal of Physiology* **22,** 103-120.

Mayerl C, Steer K, Chava A, Bond L, Edmonds C, Gould F, Stricklen B, Hieronymous T & German R. (2021). The contractile patterns, anatomy and physiology of the hyoid musculature change longitudinally through infancy. *Proceedings of the Royal Society B* **288,** 20210052.

McFarlane L, Altringham JD & Askew GN. (2016). Intra-specific variation in wing morphology and its impact on take-off performance in blue tits (Cyanistes caeruleus) during escape flights. *Journal of Experimental Biology* **219,** 1369-1377.

730

731 Mendoza E, Moen D & Holt N. (2023). The importance of comparative physiology: mechanisms,
732 diversity and adaptation in skeletal muscle physiology and mechanics. *Journal of*
733 *Experimental Biology* **226,** jeb245158.

734

735 Millard M, Uchida T, Seth A & Delp SL. (2013). Flexing computational muscle: modeling and
736 simulation of musculotendon dynamics. *Journal of Biomechanical Engineering* **135**.

737

738 Pellegrino M, Canepari M, Rossi R, D'antona G, Reggiani C & Bottinelli R. (2003). Orthologous
739 myosin isoforms and scaling of shortening velocity with body size in mouse, rat, rabbit
740 and human muscles. *The Journal of Physiology* **546,** 677-689.

741

742 Percie du Sert N, Hurst V, Ahluwalia A, Alam S, Avey MT, Baker M, Browne WJ, Clark A, Cuthill
743 IC & Dirnagl U. (2020). The ARRIVE guidelines 2.0: Updated guidelines for reporting
744 animal research. *Journal of Cerebral Blood Flow & Metabolism* **40,** 1769-1777.

745

746 Pinniger G, Ranatunga K & Offer G. (2006). Crossbridge and non‐crossbridge contributions to
747 tension in lengthening rat muscle: force‐induced reversal of the power stroke. *The*
748 *Journal of Physiology* **573,** 627-643.

749

750 Powers K, Nishikawa K, Joumaa V & Herzog W. (2016). Decreased force enhancement in skeletal
751 muscle sarcomeres with a deletion in titin. *Journal of Experimental Biology* **219,** 1311-
752 1316.

753

754 Prado LG, Makarenko I, Andresen C, Krüger M, Opitz CA & Linke WA. (2005). Isoform diversity
755 of giant proteins in relation to passive and active contractile properties of rabbit skeletal
756 muscles. *The Journal of General Physiology* **126,** 461-480.

757

758 Rajagopal A, Dembia CL, DeMers MS, Delp DD, Hicks JL & Delp SL. (2016). Full-body
759 musculoskeletal model for muscle-driven simulation of human gait. *IEEE Transactions*
760 *on Biomedical Engineering* **63,** 2068-2079.

761

762 Ramsey KA, Bakker AJ & Pinniger GJ. (2010). Fiber ‐ type dependence of stretch ‐ induced
763 force enhancement in rat skeletal muscle. *Muscle & Nerve* **42,** 769-777.

764

765 Rijkelijkhuizen J, De Ruiter C, Huijing P & De Haan A. (2003). Force/velocity curves of fast
766 oxidative and fast glycolytic parts of rat medial gastrocnemius muscle vary for
767 concentric but not eccentric activity. *Pflügers Archiv* **446,** 497-503.

768

769 Roberts TJ, Higginson BK, Nelson FE & Gabaldón AM. (2007). Muscle strain is modulated more
770 with running slope than speed in wild turkey knee and hip extensors. *Journal of*
771 *Experimental Biology* **210,** 2510-2517.

772

773 Stienen G, Versteeg P, Papp Z & Elzinga G. (1992). Mechanical properties of skinned rabbit psoas
774 and soleus muscle fibres during lengthening: effects of phosphate and Ca2+. *The Journal*
775 *of Physiology* **451,** 503-523.

776

777 Tahir U, Monroy JA, Rice NA & Nishikawa KC. (2020). Effects of a titin mutation on force
778 enhancement and force depression in mouse soleus muscles. *Journal of Experimental*
779 *Biology* **223,** jeb197038.

780

781 Team RDC. (2010). R: A language and environment for statistical computing. *(No Title)*.

782

783 Tomalka A. (2023). Eccentric muscle contractions: from single muscle fibre to whole muscle
784 mechanics. *Pflügers Archiv-European Journal of Physiology* **475,** 421-435.

785

786 Tomalka A, Rode C, Schumacher J & Siebert T. (2017). The active force–length relationship is
787 invisible during extensive eccentric contractions in skinned skeletal muscle fibres.
788 *Proceedings of the Royal Society B: Biological Sciences* **284,** 20162497.

789

790 Tomalka A, Weidner S, Hahn D, Seiberl W & Siebert T. (2020). Cross-bridges and sarcomeric
791 non-cross-bridge structures contribute to increased work in stretch-shortening cycles.
792 *Frontiers in physiology* **11,** 921.

793

794 Tomalka A, Weidner S, Hahn D, Seiberl W & Siebert T. (2021). Power amplification increases
795 with contraction velocity during stretch-shortening cycles of skinned muscle fibers.
796 *Frontiers in Physiology* **12,** 644981.

797

798 Usherwood JR. (2022). Legs as linkages: an alternative paradigm for the role of tendons and
799 isometric muscles in facilitating economical gait. *Journal of Experimental Biology* **225,**
800 jeb243254.

801

802 Warren PM, Kissane RW, Egginton S, Kwok JC & Askew GN. (2020). Oxygen transport kinetics
803 underpin rapid and robust diaphragm recovery following chronic spinal cord injury. *The*
804 *Journal of Physiology*.

805

806 Weidner S, Tomalka A, Rode C & Siebert T. (2022). How velocity impacts eccentric force
807 generation of fully activated skinned skeletal muscle fibers in long stretches. *Journal of*
808 *Applied Physiology*.

809

810 Woledge R, Curtin N & Homsher E. (1985). Mechanics of contraction. *Energetic Aspects of Muscle*
811 *Contraction Academic Press, London***,** 47-71.

812

813
814

Conserved mammalian muscle mechanics during eccentric contractions

Roger W. P. Kissane[1*] and Graham N. Askew[2*]

[1] Department of Musculoskeletal & Ageing Science, University of Liverpool, The William Henry Duncan Building, 6 West Derby Street, Liverpool L7 8TX, UK

[2] School of Biomedical Sciences, University of Leeds, UK

*Correspondence to: r.kissane@liverpool.ac.uk and g.n.askew@leeds.ac.uk

Funding: This research was supported by a BBSRC Project Grant (BB/R016917/1) to GNA. This work was also supported by an internal funding scheme funded by the Wellcome Trust Institutional Strategic Support Fund grant (204822/Z/16/Z) and awarded to RWPK by the Faculty of Health and Life Sciences, University of Liverpool.

Running Title: Conserved mammalian muscle mechanics during eccentric contractions

Key words: Force Velocity, Muscle Mechanics, Scaling, Titin, Lengthening

Appendix

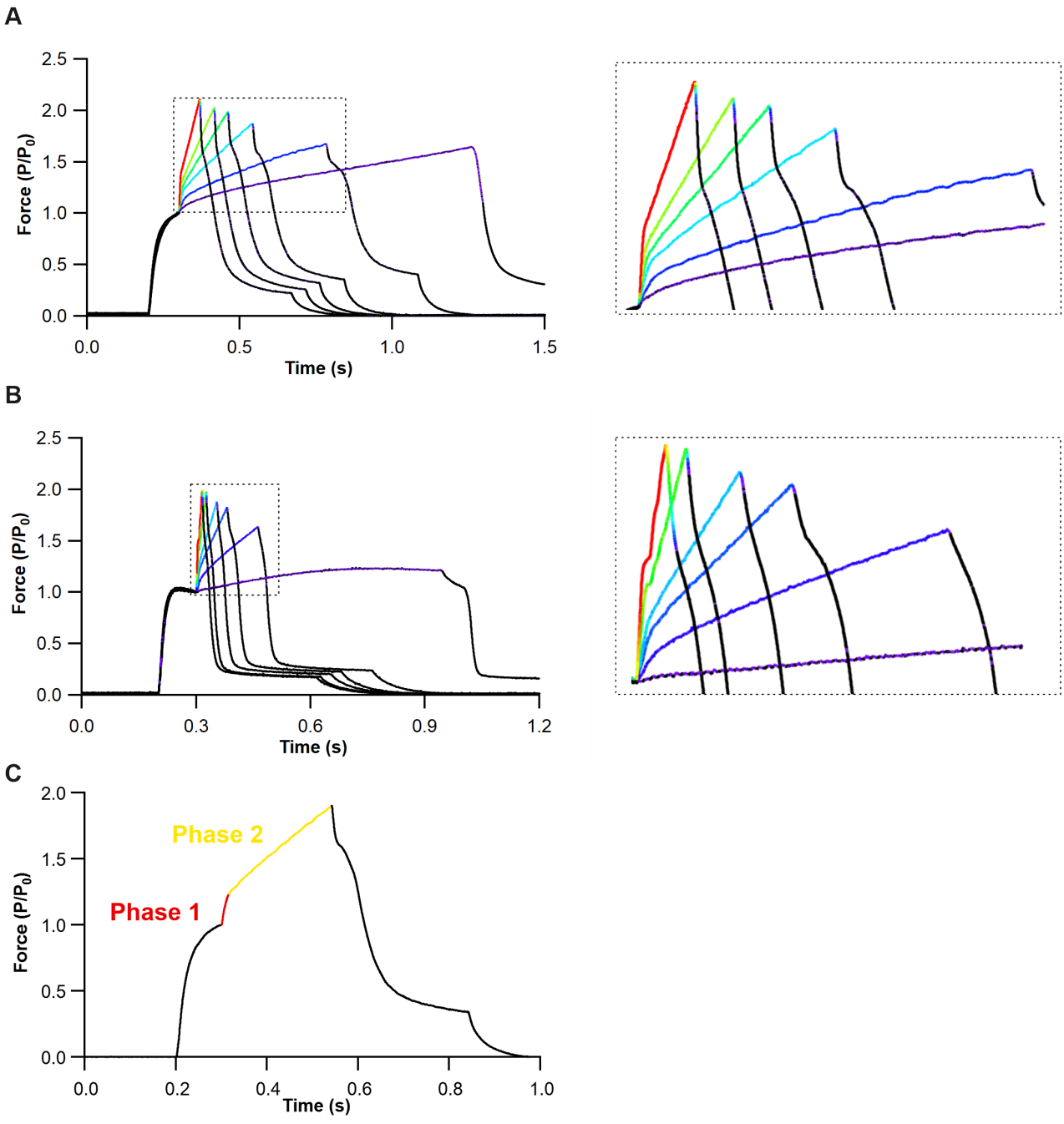

833

834 **Appendix Figure 1. Example eccentric plots.** Isovelocity lengthening from a single animal, for the
835 soleus (A) and extensor digitorum longus (B). Expanded regions emphasise the two-phase response
836 of both muscles during lengthening. These comprise of a phase of rapid force-development (phase-
837 1) and a phase of slow force-development (phase-2) (C).

838

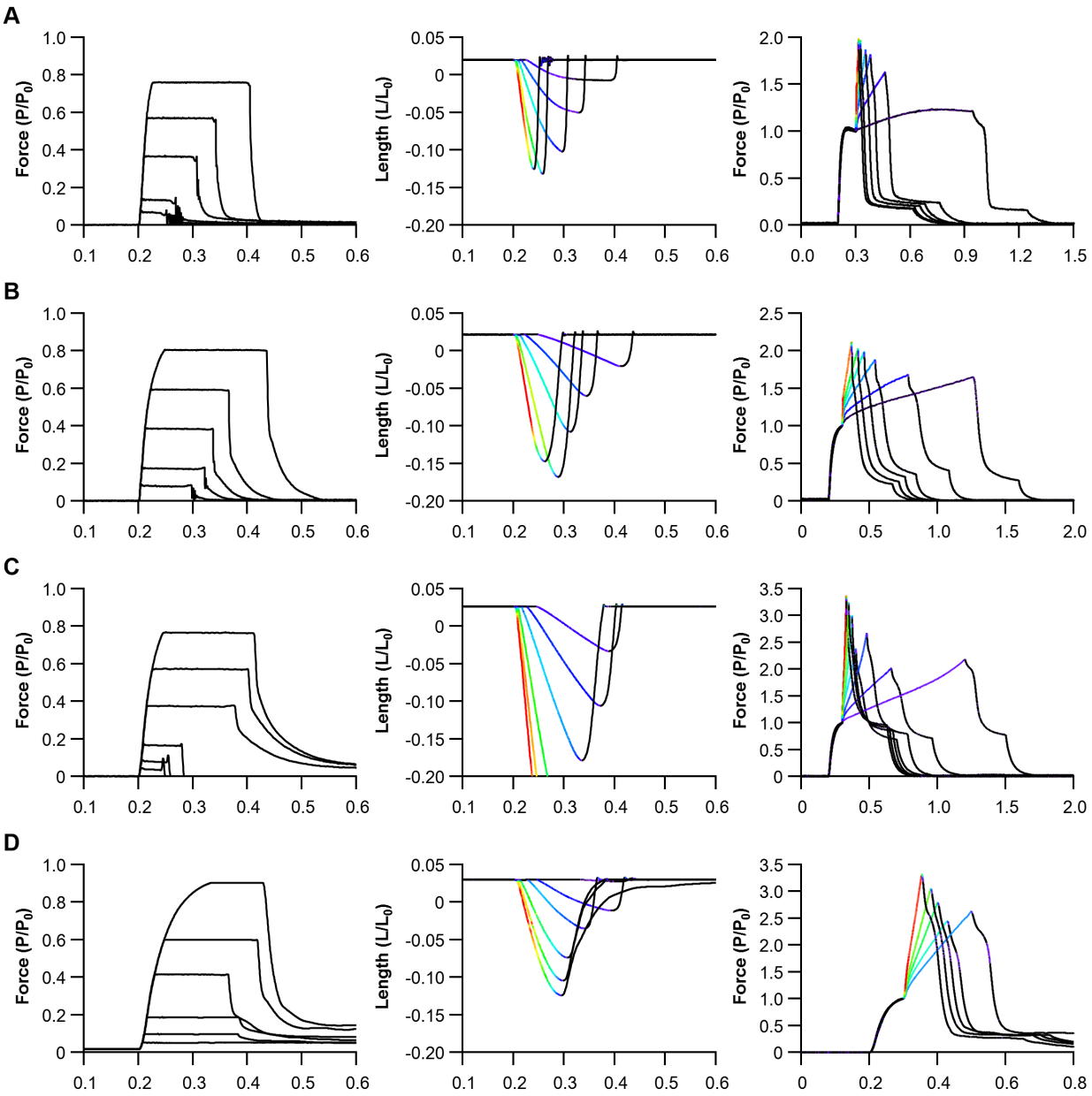

Appendix Figure 2. Example concentric and eccentric force plots. Example force (left column) and length (middle column) profiles during isotonic shortening (concentric) experiments for the mouse soleus (A), mouse extensor digitorum longus (B), rat diaphragm (C) and rabbit digastric muscle (D). Example isovelocity lengthening (eccentric) force profiles for these muscles are presented in the right-hand column. Heat map colours correspond the velocity of either muscle shortening or lengthening.

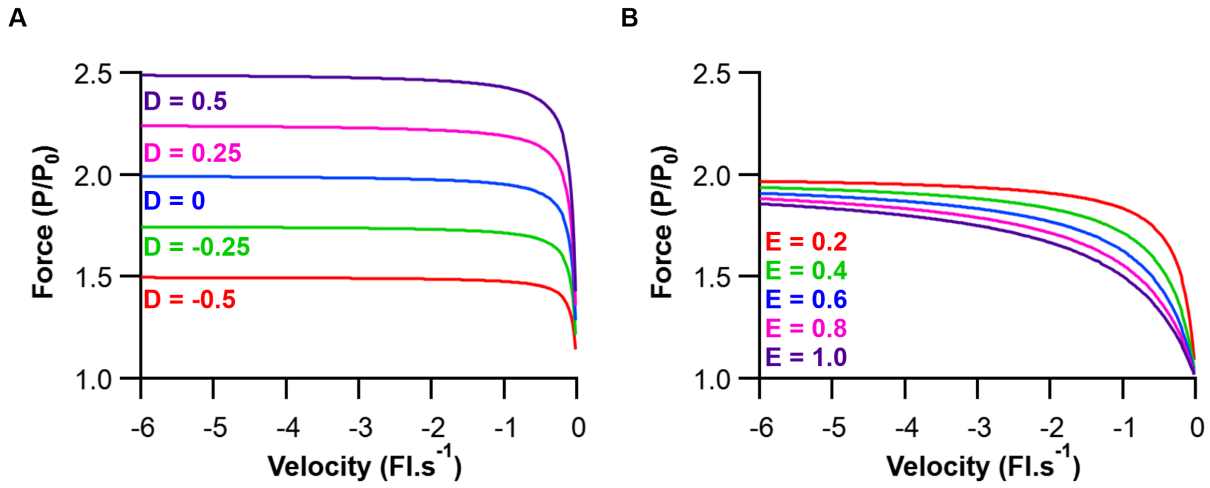

847

848 **Appendix Figure 3. Coefficients of the eccentric force-velocity equation.** Changes in coefficient
849 D alter the plateau height of the eccentric force-velocity fit (A) while changes in the E coefficient
850 vary the curvature of this relationship (B). Coefficient E was fixed at 0.05 in (A) while coefficient D
851 was fixed at 0 in (B).

852

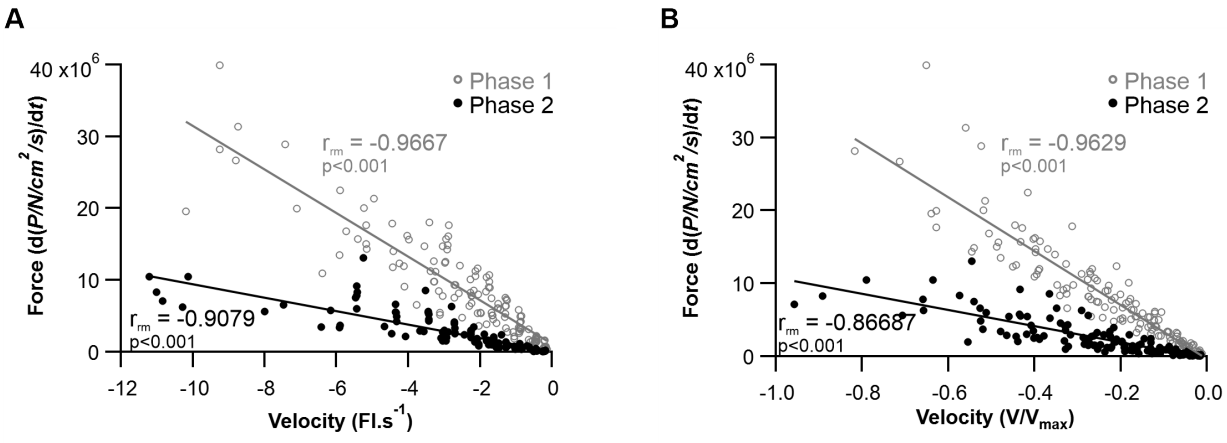

853

854 **Appendix Figure 4. Pooled rate of force development relative to PCSA.** Pooled rate of force
855 development as a function of absolute lengthening velocity (A) and normalised lengthening velocity
856 (B) across phase one (grey) and phase two (black) (B) of the isovelocity lengthening relationship. *
857 P<0.05, **P<0.01, ***P<0.001.

858

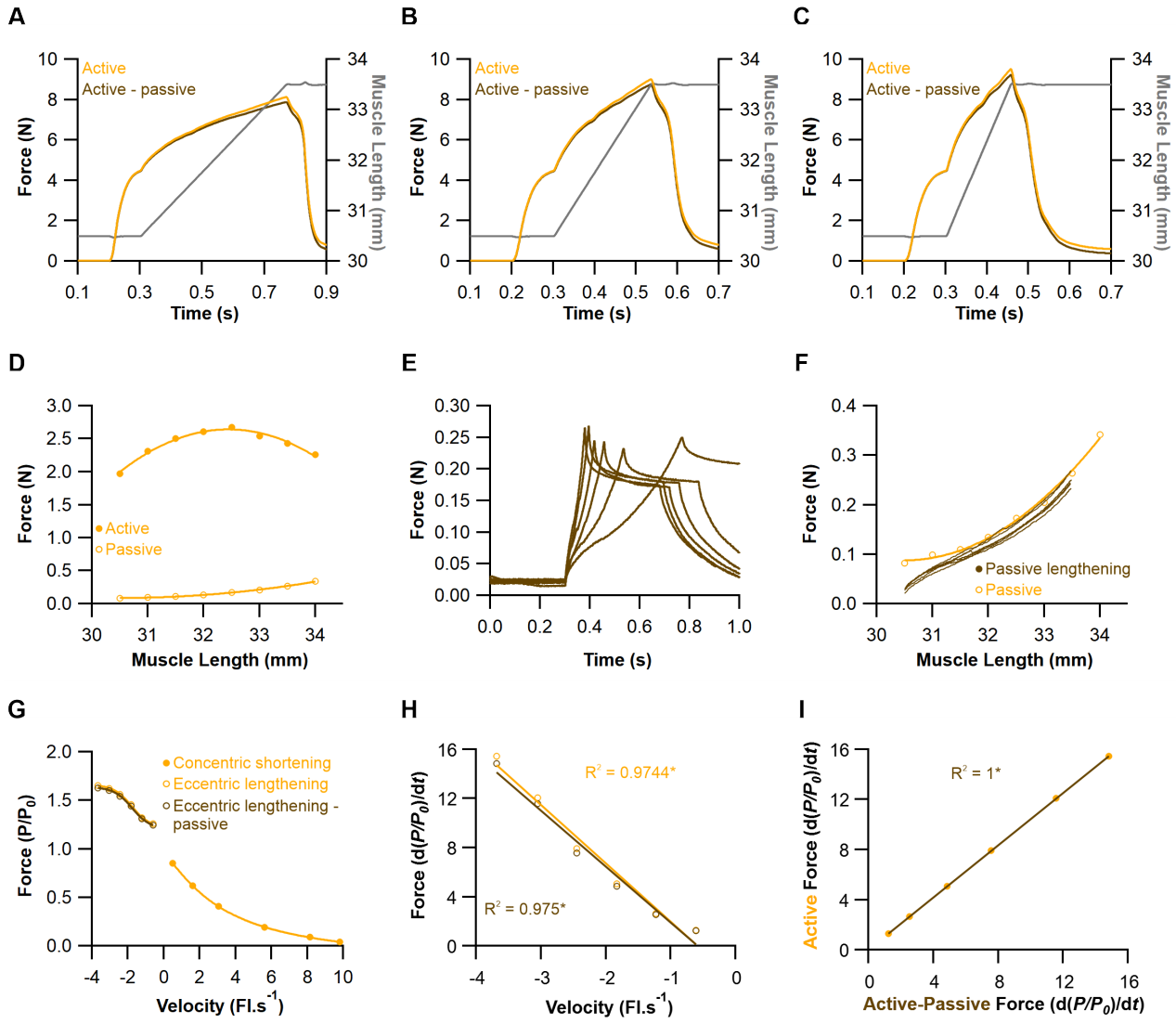

Appendix Figure 5. Passive muscle properties during muscle lengthening of the rabbit digastric muscle. Example muscle forces during lengthening at -0.61 (A), -1.22 (B) and -1.83 Fl s^{-1} (C) for absolute forces (orange) and active forces minus passive forces (brown) from a single digastric muscle. Muscle specific isometric twitch force-length relationship (D). Muscle forces during six passive lengthening ramps at different velocities (brown) (E). Passive force length data (taken from D) are plot again passive ramp forces (taken from E) which overlap with the isometric passive force (orange) (F). These data highlight the independence of passive force properties to the velocity of stretch. Eccentric (unfilled circles) and concentric (filled circles) force-velocity relationship, with active (orange) and active minus passive (brown) eccentric plots showing a similar relationship (G). The correlation for the phase-2 d(P/P_0)/dt *vs.* velocity shows a comparable rate of force development for both the active (orange) and the active minus the passive forces (brown) (H) and when correlated together show a linear relationship (I).